Primates (2019) 60:401–419
https://doi.org/10.1007/s10329-019-00740-1

ORIGINAL ARTICLE

Shape variation in the facial part of the cranium in macaques and African papionins using geometric morphometrics

Takeshi Nishimura[1] · **Naoki Morimoto**[2] · **Tsuyoshi Ito**[1]

Received: 29 May 2019 / Accepted: 6 August 2019 / Published online: 29 August 2019

Abstract

Macaques are one of the most successful nonhuman primates, and morphological distinctions from their close relatives, African papionins, are easily detected by the naked eye. Nevertheless, evolutionary allometry often accounts for a large amount of the total variation and potentially hides and precludes the detection of morphological distinctions that exist between macaques and African papionins, thus distorting their phyletic comparison. Geometric morpgometric analyses were performed using landmark coordinates in cranial samples from macaques ($N=$ 135) and African papionins ($N=$ 152) to examine the variation in their facial shape. A common allometric trend was confirmed to represent a moderately long face in macaques as being small-to-moderate-bodied papionins. Macaques possessed many features that were distinct from those of African papionins, while they simultaneously showed a large intrageneric variation in every feature, which precluded the separation of some groups of macaques from African papionins. This study confirmed that a moderately smooth sagittal profile is present in non-Sulawesi macaques. It also confirmed that a well-developed anteorbital drop is distinct in *Mandrillus* and *Theropithecus*, but it showed that *Papio* resembles macaques regarding this feature. This finding showed that apparently equivalent features which can be detected by the naked eye were probably formed by different combinations of the principal patterns. It should be noted that the differences detected here between macaques and African papionins are revealed after appropriate adjustments are made to eliminate the allometric effects over the shape features. While landmark data sets still need to be customized for specific studies, the information provided by this article is expected to help such customization and to improve future phyletic evaluation of the fossil papionins.

Keywords Papionins · *Macaca* · Sulawesi macaques · Geometric morphometrics · Evolutionary allometry

Introduction

The Old World monkey tribe Papionini is one of the most successful groups among nonhuman primates. This tribe likely separated from the tribe Cercopithecini in the Middle to Late Miocene (Perelman et al. 2011; Pozzi et al. 2014). Subsequently, the two subtribes of Papionina and Macacina arose in the Late Miocene in Africa (Harris 2000; Pozzi et al. 2014; Raaum et al. 2005; Roos et al. 2019; Springer et al. 2012; Tosi et al. 2003). Papionina includes six extant genera, i.e., *Mandrillus*, *Cercocebus*, *Papio*, *Theropithecus*, *Lophocebus*, and *Rungwecebus* (Fleagle 2013). The extant forms are distributed across the African continent, with the exception of the *Papio hamadryas* population, which also inhabits the coastal areas of the Red Sea in the Arabian Peninsula (Fleagle 2013). They are often termed "African papionins" (Strasser and Delson 1987). Papioninans diversified in abundant number and achieved successful radiation at the genus level under the diverse ecological environmental fluctuations of the Plio-Pleistocene in Africa, as evidenced by the extinct *Parapapio*, *Gorgopithecus*, *Dinopithecus*, *Soromandrillus*, *Pliopapio*, and *Procercocebus* (Frost 2001; Gilbert 2007; 2013; Jablonski and Frost 2010; Pugh and Gilbert 2018; Roos et al. 2019; Szalay and Delson 1979). Further, *Theropithecus* occurred in Eurasia, but its

Electronic supplementary material The online version of this article (https://doi.org/10.1007/s10329-019-00740-1) contains supplementary material, which is available to authorized users.

✉ Takeshi Nishimura
nishimura.takeshi.2r@kyoto-u.ac.jp

[1] Primate Research Institute, Kyoto University, 41-2 Kanrin, Inuyama, Aichi 484-8506, Japan

[2] Laboratory of Physical Anthropology, Graduate School of Science, Kyoto University, Kitashiralkawa-Oiwakecho, Sakyo, Kyoto 606-8502, Japan

Eurasian descendants are extinct (Belmaker 2010; Delson 1993; Gibert et al. 1995; Gupta and Sahni 1981; Roberts et al. 2014). Currently, *Papio* is a nonhuman primate that has achieved successful adaptation in varied habitats of Africa (Gilbert 2013; Gilbert et al. 2018; Jolly 1967). Macacina comprises the single extant genus *Macaca*, i.e., macaques (Fleagle 2013). Macaques are distributed in tropical to temperate Asia and Northern Africa. Macacinans dispersed into Europe from Africa during the latest Miocene (Alba et al. 2014; 2018; Delson 2000; Strasser and Delson 1987) and were distributed widely in Eurasia. They achieved successful radiation at the species level in the Late Pliocene and Pleistocene of Asia, but disappeared from Europe and high latitudes at the end of the Pleistocene (Delson 1980; Fooden 1980; Roos et al. 2019). Two additional large-bodied papionins, *Procynocephalus* and *Paradolichopithecus*, have been reported from the Middle Pliocene to the Early Pleistocene in Eurasia. The two genera are regarded as being phylogenetically close (Jablonski 2002; Kostopoulos et al. 2018; Szalay and Delson 1979), and both are usually considered as extinct forms of Macacina (Jablonski 2002; Nishimura et al. 2014; Szalay and Delson 1979). Nevertheless, some of the specimens show several features that are found in extant *Papio* (Maschenko 1994; 2005; Takai et al. 2008), and the phyletic position and relationship of specimens assigned to each genus remains under dispute (Kostopoulos et al. 2018; Nishimura et al. 2007; 2009; Takai et al. 2008).

Morphological distinctions in skulls are easily found between the extant African papionins and macaques using the naked eye (Strasser and Delson 1987). The large-bodied African papionins (*Mandrillus*, *Papio*, and *Theropithecus*) have a long muzzle with a well-developed anteorbital concavity (drop) and distinctive maxillary fossae, while the small-bodied forms (*Cercocebus*, *Lophocebus*, and *Rungwecebus*) have a short and steep face with distinctive suborbital fossae (Fleagle 2013; Gilbert et al. 2009; Springer et al. 2012; Strasser and Delson 1987). Macaques exhibit a size range that overlaps with the small-bodied African papionins and the lower end of the range of the large-bodied taxa (Fleagle 2013; Singleton 2002), have a moderately long and rounded dorsal surface of the muzzle, and usually lack maxillary and suborbital fossae (Gilbert et al. 2009; Jablonski 2002; Szalay and Delson 1979). Nevertheless, some of these more obvious morphological distinctions between papionins can be explained in terms of evolutionary allometric scaling (Albrecht 1978; Collard and O'Higgins 2001; Frost et al. 2003; Gilbert et al. 2009; Gilbert and Rossie 2007; Kieser and Groeneveld 1987; Leigh 2007; Leigh et al. 2003; Pan and Oxnard 2000; Singleton 2002). In fact, a major and well-known allometric trend is that large-bodied papionins exhibit a proportionally low, long, and narrow face (Freedman 1962; Frost et al. 2003; Gilbert and Grine 2010; Ito et al. 2011; 2014; Leigh et al. 2003; Shea 1983; Singleton 2002; 2004). Such major evolutionary allometry often accounts for a large amount of the total variation and, thus, can hide and preclude the detection of morphological distinctions that exist between macaques and African papionins.

Evolutionary allometry is an artifact that has confused the taxonomy and phylogeny of African papionins in the past. For the past 25 years, molecular analyses have recognized two clades, one comprising *Mandrillus* and *Cercocebus*, and the other comprising *Papio*, *Theropithecus*, *Lophocebus*, and *Rungwecebus* (Disotell 1994; 1996; 2000; Harris 2000; Liedigk et al. 2014; Pugh and Gilbert 2018; Tosi et al. 2003). This view is currently accepted by most scholars. In contrast, the traditional coding of morphological characters often supported a different view comprising the two clades: the large-bodied (*Mandrillus*, *Papio*, and *Theropithecus*) and the small-bodied (*Cercocebus* and *Lophocebus*) forms (Collard and Wood 2001; Gilbert et al. 2009; Szalay and Delson 1979). This traditional view probably reflects a discontinuous distinction in size between the two forms of extant African papionins, and is almost certainly influenced by a common allometric trend in papionins; i.e., larger-bodied forms have a long face, while small-bodied ones have a short face (Collard and Wood 2001; Frost et al. 2003; Gilbert et al. 2009; Singleton 2002). After the elaboration of a coding system in which quantitative and qualitative characters were more precisely size-corrected, i.e., from which allometric effects were eliminated, this incongruence between molecular and morphological phylogenies was successfully solved (Gilbert et al. 2009; Gilbert and Rossie 2007; Gilbert et al. 2011). These findings suggest that distinctions not detectable by the naked eye are revealed between the two subtribes after adjusting for major allometric effects on cranial shape.

Many efforts have been made to detect evolutionary allometry and the features that are not heavily influenced by scaling in papionins (Collard and O'Higgins 2001; Frost et al. 2003; Gilbert 2013; Gilbert and Grine 2010; Leigh 2007; Leigh et al. 2003; Singleton 2002; 2004; 2012). Those past studies usually aimed to examine the variation within African papionins using a limited sample from a few species of *Macaca*. Extant macaques are assigned to a single genus, but they are successful in adaptive radiation and consist of approximately 20 extant species (Fleagle 2013; Roos et al. 2019). They are classified into four groups termed "species groups", i.e., the *sylvanus*, *silenus*, *sinica*, and *fascicularis* groups, based on the morphology of the genitalia and crania, biogeography, fossil records, and molecular evidence (Delson 1980; Fooden 1976; 1980; Li et al. 2009; Li and Zhang 2005; Tosi et al. 2003; 2000). The *sylvanus* group first diverged from the remaining clades in the Late Miocene, followed by the diversification of the *silenus* group from the *sinica*/*fascicularis* groups in Asia in the Late Pliocene (Delson 1980; Li et al. 2009; Liedigk et al. 2014; Pozzi et al. 2014; Roos et al. 2019). Their diversification at the level of

the species groups occurred in almost the same era as did the diversification of genera in extant African papionins. The macaques that inhabit Sulawesi Island are members of the *silenus* group and are probably a sister clade of *Macaca nemestrina* from Borneo; however, they are quite distinct from the other non-Sulawesi macaques regarding facial shape (Albrecht 1978; Fooden 1969; 1976). Because of these distinct properties, they are often excluded from examinations of morphological variation and phyletic analyses in macaques (e.g., Ito et al. 2014). Thus, this large intrageneric variation in the morphology of extant macaques needs to be evaluated for comparison with the intergeneric variation in African papionins for a better understanding of evolutionary allometry in this tribe and of the morphological distinctions between macaques and African papionins.

Three-dimensional (3-D) geometric morphometrics using the Procrustes method of superimposition of landmark coordination is one of the most effective approaches for extracting variation patterns that are affected by evolutionary allometry (Collard and O'Higgins 2001; Frost et al. 2003; Ito et al. 2011; 2014; O'Higgins and Collard 2002; O'Higgins and Jones 1998; Singleton 2002). A generalized Procrustes analysis (GPA) approach eliminates the scale, translational, and rotational differences of the coordinate data of the landmarks among subjects. The coordinate data of each specimen are usually scaled by its centroid size (CS). The CS and GPA-scaled coordinates represent surrogates of size and shape, respectively. Principal components analysis (PCA) of the Procrustes-aligned coordinates is often used to summarize major variations in shape within a given sample. Any principal component (PC) that is highly correlated with CS is regarded as representing a variation pattern that is affected by allometry. Here, we used this approach on a large sample of macaques, representative of their intrageneric variation, to examine the distinctions in facial shape between macaques and African papionins.

Materials and methods

We examined dry bone specimens that included 287 crania of extant papionins: 37 crania of *Cercocebus*, 28 of *Mandrillus*, 30 of *Lophocebus*, 19 of *Theropithecus*, 38 of *Papio*, and 135 of *Macaca* (Table 1). Here, we dealt with Sulawesi macaques separately as a group that was independent from the *silenus* group. The specimens of *Macaca* comprised 6 *sylvanus* group crania, 25 *silenus* group crania, 33 *sinica* group crania, 33 *fascicularis* group crania, and 38 Sulawesi macaques crania (Table 1). The *sylvanus* group comprises only *Macaca sylvanus*; thus its sample size was small. The specimens used here were housed at the Field Museum of Natural History, Chicago, IL, USA; the American Museum of Natural History, New York, NY, USA; the National

Table 1 Specimens used in this study

Groups	Total	Male	Female
African papionins	152	91	61
Cercocebus	37	20	17
Cer. agilis	11	6	5
Cer. galeritus	3	2	1
Cer. atys	9	4	5
Cer. torquatus	13	8	5
Cer. cf. *torquatus*	1	0	1
Mandrillus	28	19	9
Man. leucophaeus	11	7	4
Man. sphinx	17	12	5
Lophocebus	30	15	15
Lop. albigena	4	2	2
Lop. aterrimus	7	4	3
Lop. johnstoni	16	8	8
Lop. cf. *albigena*	3	1	2
Theropithecus gelada	19	14	5
Papio	38	23	15
Pap. anubis	8	4	4
Pap. cynocephalus	8	4	4
Pap. hamadryas	6	6	0
Pap. papio	7	5	2
Pap. ursinus	9	4	5
Macaques (*Macaca*)	135	75	60
Non-Sulawesi macaques	97	57	40
Sylvanus group	6	2	4
Mac. sylvanus	6	2	4
Silenus group	25	16	9
Mac. silenus	2	1	1
Mac. leonina	6	4	2
Mac. nemestrina	14	10	4
Mac. pagensis	3	1	2
Sinica group	33	22	11
Mac. sinica	4	3	1
Mac. radiata	4	2	2
Mac. arctoides	4	3	1
Mac. assamensis	13	9	4
Mac. thibetana	8	5	3
Fascicularis group	33	17	16
Mac. fascicularis	10	5	5
Mac. mulatta	9	4	5
Mac. cyclopis	4	2	2
Mac. fuscata	10	6	4
Sulawesi macaques	38	18	20
Mac. brunnescens	4	1	3
Mac. hecki	10	5	5
Mac. maura	4	2	2
Mac. nigra	9	5	4
Mac. ochreata	3	1	2
Mac. tonkeana	8	4	4
Total	287	156	121

Museum of Natural History, Washington, DC, USA; and the Primate Research Institute of Kyoto University, Inuyama, Japan. They all belonged to adult individuals with the upper third molar fully or almost erupted, and they had no pathological traits in the cranium, as assessed using the naked eye. Crania of each genus of African papionins and each group of macaques were sampled both from wild and captive sources.

3-D coordinates representing 31 landmarks in the facial part of the cranium were acquired using a 3-D digitizer (MicroScribe MX, Immersion Corp., San Jose, CA, USA; Table 2, Fig. 1). Measurements were taken only on the left side; for 12 specimens with broken left sides, however, the horizontal reversals of the right side measurements were used. For eight specimens, one or two missing landmarks were estimated by mapping weighted averages from the complete data set onto the missing specimen using the "Morpho" package (Schlager 2017) in R statistical software (R Development Core Team 2016).

All specimens were digitized twice by a single observer (T.I.). The measurement errors for shape and size were evaluated by analysis of variance (ANOVA) using the "geomorph" (Adams et al. 2019) and "car" (Fox and Weisberg 2018) packages in R, respectively. The individual variations in shape and size were much larger than the measurement errors [shape: $F = 116.19$, $P = 0.001$ (randomized residual permutation procedure with 999 iterations); size: $F = 35909$, $P < 0.001$]. The mean values of the repeated measures were used in the subsequent analyses.

While the actual landmarks were taken only on the left side, geometric morphometric analyses were performed for the entire face. The landmarks on the right side were obtained by flipping the landmarks on the left side relative to the midsagittal plane. To define the midsagittal plane, a least-squares plane was calculated using the landmarks labeled as "midsagittal" in Table 2. Thus, the landmark configuration analyzed in this study was symmetrical relative to the midsagittal plane. The landmark data were then analyzed using geometric morphometrics methods (Bookstein 1991). The landmark coordinates of each specimen were scaled by CS. Differences in position and rotation were corrected using the GPA. Procrustes residuals were then analyzed by PCA to identify patterns of shape variation in the sample.

To visualize each principal pattern of shape variation, we used the methods proposed by Zollikofer and Ponce de León (Zollikofer and Ponce de León 2002). The shape changes along each PC were visualized as a deformation of the 3-D surface model of the facial part of the cranium, but not as the deformation of the line framework with landmarks that inevitably illustrate the movement of each landmark that was not of interest here. The deformation of the surface model according to the different landmark configurations was calculated using the thin plate spline function. The movement of each triangle in the surface model according to the deformation from one model to the other was decomposed into two orthogonal factors, i.e., local normal and tangent. The movements along the normal and tangent directions were visualized by false-color and vector mapping. Here, we generated the surface model from the computed tomographic scans of a female specimen of *Macaca nemestrina* (specimen ID #3054, Primate Research Institute of Kyoto University; scan data PRICT ID #721 available at http://dmm.pri.kyoto-u.ac.jp/dmm/).

Statistical analyses were performed using a custom script written in the R. Any PC representing an evolutionary allometric trend was confirmed by a least-squares regression analysis of the scores of each PC against the natural logarithm of CS (logCS). Bartlett's test does not support the homoscedasticity of scores between sexes and/or groups (Table 3). Hence, non-parametric Mann–Whitney tests were performed using the "coin" package (Hothorn et al. 2006) in R to examine the significance of differences in the score of each PC between sexes in each group, excluding the *sylvanus* group. Kruskal–Wallis tests with a post hoc Steel–Dwass test were conducted using the "coin" package (Hothorn et al. 2006) and a custom script in R, to examine the significance of differences between groups and between each pair of groups. The figures were prepared using the "ggplot2" package (Wickham 2016) and a custom script in R.

Results

The PCA revealed that the first five PCs accounted for > 80% of the total variation in facial shape (Table 4). Each of the succeeding PCs summarized < 2.0% of the total variation (Table 4). The first five PCs were evaluated here. The Kruskal–Wallis test confirmed that logCS and the scores of the five PCs were significantly different between the genera/groups ($P < 0.001$). We descried the differences between each pair of the groups using the post hoc Steel–Dwass test, as follows.

The first principal component (PC1) summarized 57.8% of the total variation in shape (Table 4). The PC1 score was significantly and highly correlated with logCS (Table 5; $P < 0.001$, $r^2 = 0.8373$). Figure 2a depicts this significant linear relationship. This means that the shape variation summarized by this PC represents an evolutionary allometric trend in this tribe. The large-bodied African papionins (*Papio*, *Theropithecus*, and *Mandrillus*) had high scores, and small-bodied African papionins (*Lophocebus* and *Cercocebus*) had low scores. In comparison, Macaques (*Macaca*) had intermediate scores, while they overlapped the small-bodied African papionins and the lower end of the large-bodied *Papio* (Fig. 2). Sulawesi macaques had slightly higher scores than the other macaques (Fig. 2). They had a significantly higher score

Table 2 Definitions fof landmarks used in this study

Abbreviation	Position	Definition	Reference
PRS	Midsagittal	Prosthion: antero-inferior point on projection of premaxilla between central incisors	Standard, e.g., Cardini et al. (2007)
PRS2	Lateral	Prosthion2: antero-inferior-most point on pre-maxilla, equivalent to prosthion but between central and lateral incisors	Frost et al. (2003)
LIA	Lateral	Posterior-most point of lateral incisor alveolus	Cardini et al. (2007)
PMS	Lateral	The point where premaxillary suture crosses alveolar marigin	Frost et al. (2003)
ACA	Lateral	Anterior-most point of canine alveolus	Cardini et al. (2007)
MP3	Lateral	Mesial P3: most mesial point on P^3 alveolus, projected labially onto alveolar margin	Frost et al. (2003)
MM1	Lateral	Mesial M1: contact points between P^4 and M^1, projected labially onto alveolar margin	Cardini et al. (2007)
MM3	Lateral	Mesial M3: contact points between M^2 and M^3, projected labially onto alveolar margin	Cardini et al. (2007)
DM3	Lateral	Distal M3: posterior midpoint onto alveolar margin of M^3	Frost et al. (2003)
PMA	Lateral	Most posterior point of maxilla at the border with the palatine	Ito et al. (2014)
PMI	Lateral	The point where premaxillary suture crosses the infero-lateral marigin of incisive foramen	The pesent study
PIF	Midsagittal	Incisivion: posterior-most point of incisive foramen	Standard, e.g., Cardini et al. (2007)
MXP	Midsagittal	Meeting point of maxilla and palatine along midline	Cardini et al. (2007)
GPF	Lateral	Most posterior point on the margin of greater palatine foramen	Cardini et al. (2007)
CPP	Midsagittal	Point of maximum curvature on the posterior edge of the palatine	Cardini et al. (2007)
PNS	Midsagittal	Tip of posterior nasal spine	Cardini et al. (2007)
NSP	Midsagittal	Nasospinale: inferior-most midline point of piriform aperture	Standard, e.g., Cardini et al. (2007)
WPA	Lateral	Point corresponding to largest width of piriform aperture	Cardini et al. (2007)
NPM	Lateral	Meeting point of nasal and pre-maxilla on margin of piriform aperture	Cardini et al. (2007)
RHI	Midsagittal	Rhinion: most anterior midline point on nasals	Standard, e.g., Cardini et al. (2007)
NAS	Midsagittal	Nasion: midline point on fronto-nasal suture	Standard, e.g., Cardini et al. (2007)
GLA	Midsagittal	Glabella: most forward projecting midline point of frontals at the level of the supraorbital ridges	Standard, e.g., Cardini et al. (2007)
DCR	Lateral	Dacryon: most superior point of the lacrimomaxillary suture (intersection with frontal bone)	Standard, e.g., Cobb and O'Higgins (2007)
OPF	Lateral	Inferior margin of optic foramen	The pesent study
IST	Lateral	Point on inferior margin of supraorbital torus (superior margin of orbit) at middle of orbit	Frost et al. (2003)
FRO	Lateral	Frontomalare orbitale: where frontozygomatic suture crosses inner orbital rim	Standard, e.g., Cardini et al. (2007)
ZMS	Lateral	Zygo-max superior: antero-superior point of zygomaticomaxillary suture taken at orbit rim	Frost et al. (2003)
ZMI	Lateral	Zygo-max inferior: antero-inferior point of zygomaticomaxillary suture	Frost et al. (2003)
CZA	Lateral	Maximum curvature of anterior upper margin of zygomatic arch	Cardini et al. (2007)
ZTS	Lateral	Zygo-temp superior: superior point of zygomatico-temporal suture on lateral face of zygomatic arch	Frost et al. (2003)
FRT	Lateral	Frontomalare temporale: where frontozygomatic suture crosses lateral edge of zygoma	Standard, e.g., Cardini et al. (2007)

than the *sinica* and *fascicularis* groups; however, Sulawesi macaques were not significantly different in size from non-Sulawesi macaques (Tables 6, 7; Figs. 2, 3). Male subjects had a significantly higher score than did females in every group, with the exception of *Theropithecus* (Table 7, Fig. 2b), which reflects the fact that males are larger in size than females (Table 8, Fig. 3). The PC1 score was not significantly different between sexes, and male subjects overlapped females in *Theropithecus*, while the logCS was significantly different between sexes. Figure 4 and Online Resource 1 depict the principal pattern of shape variation provided by PC1. Lower scores (i.e., decreasing logCS) are characterized by a proportionally short and wide facial shape with a long nasal aperture, a relatively large and

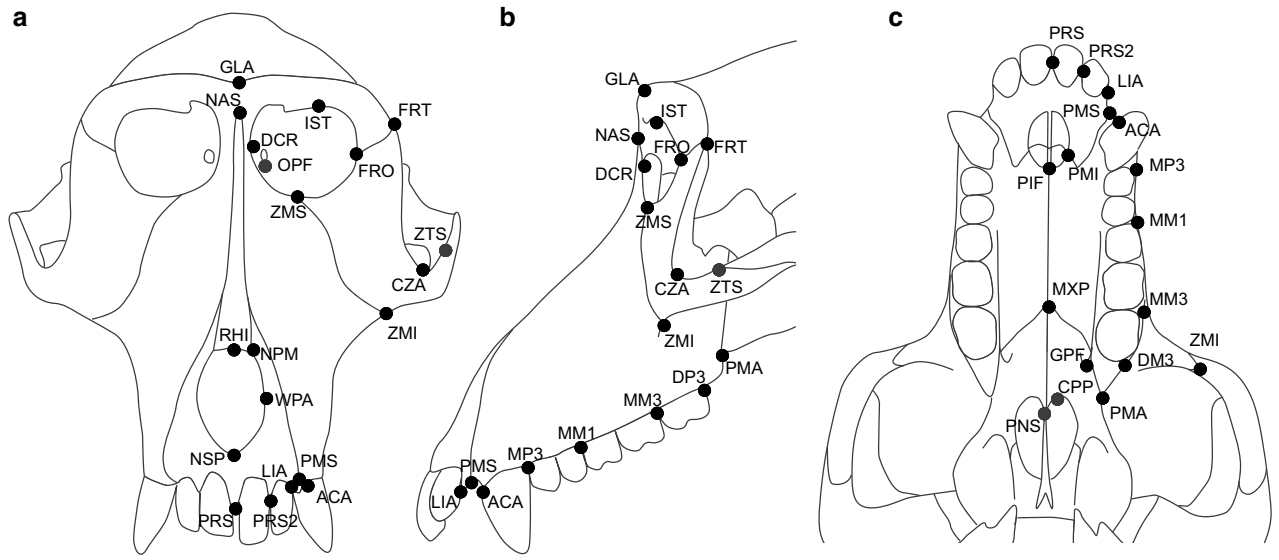

Fig. 1 Landmarks on the surface of the face used in this study. **a** Frontal view, **b** lateral view, and **c** occlusal view. See Table 2 for the definitions of the abbreviations

Table 3 Homogeneity of variance by Bartlett's test

	logCS	PC1	PC2	PC3	PC4	PC5
Group	0.0000**	0.0079*	0.0920	0.0000**	0.0026*	0.0000**
Sex	0.0079*	0.2685	0.0059*	0.2288	0.2696	0.0000**

logCS and some PCs demonstrate significant deviation from normal distribution

logCS logarithmic centroid size

p values with a significance code** < 0.001; * < 0.01

Table 4 Proportions of PCA

	Proportion	Cumulative
PC1	0.578	0.578
PC2	0.101	0.679
PC3	0.081	0.760
PC4	0.031	0.790
PC5	0.027	0.817
PC6	0.018	0.835

Table 5 Regression analyses of PC scores and logarithmic centroid size (logCS)

	Slope	Intercept	R^2	*F* statistic	*p* value
PC1	0.8967	−2.1538	0.8373	1467	0.0000**
PC2	0.0004	−0.0010	0.0000	0.000	0.9867
PC3	−0.0917	0.2204	0.0624	18.97	0.0000**
PC4	−0.0164	0.0394	0.0053	1.519	0.2189
PC5	0.0258	−0.0620	0.0152	4.385	0.0372

p values with a significance codes ** < 0.001

vertical orbit, and a reduced angle between the upper face and the short nasal roof, and higher scores (i.e., increasing logCS) are characterized by a proportionally long and narrow facial shape with a short nasal aperture, a relatively small and posteriorly sloping orbit, and a large angle between the upper face and the long nasal roof.

The second principal component (PC2) summarized 10.1% of the total variation (Table 4). The PC2 score was not significantly correlated with logCS ($P = 0.9867$, $r^2 < 0.00005$; Table 5, Fig. 5a) and was not significantly different between sexes in each group (Table 8, Fig. 5b). *Theropithecus* had distinctively high scores and was significantly different from the other groups of papionins, with the exception of the *sylvanus* group (Table 9, Fig. 5). Macaques had the second highest scores between *Theropithecus* and the other African papionins (Fig. 5). The PC2 score was significantly different in most pairs of macaques and African papionins (Table 9, Fig. 5). The *sylvanus* group had slightly higher scores than did the other macaques and was not significantly different from *Theropithecus*, while the *silenus* group had a lower score and was not significantly different from *Papio* and *Cercocebus* (Table 9, Fig. 5). The PC2

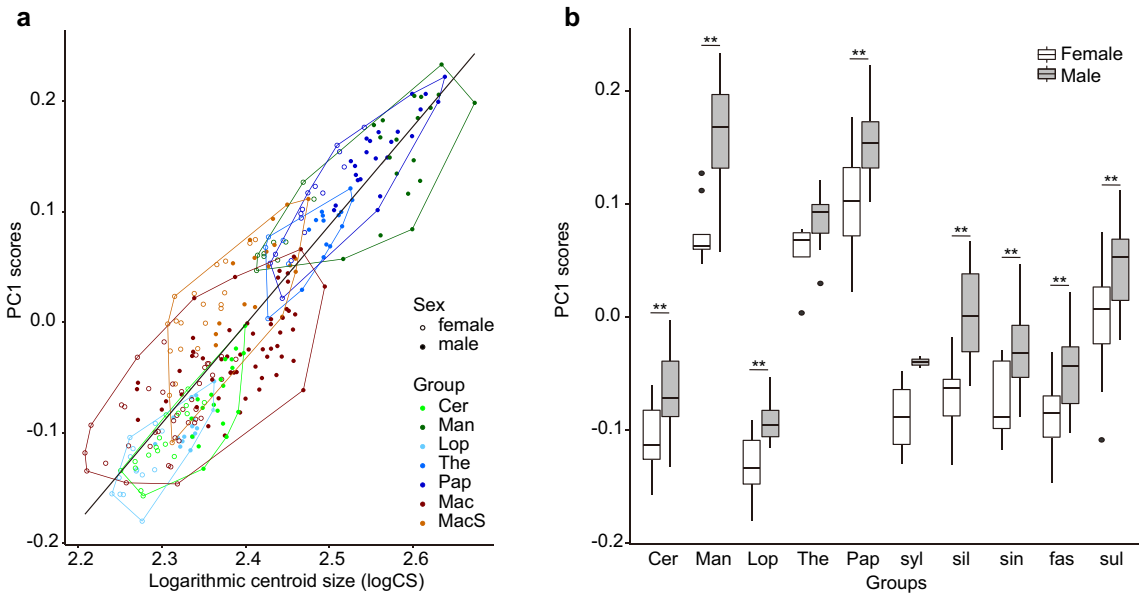

Fig. 2 Scatter (**a**) and box (**b**) plots of PC1 scores. The solid line in black represents the regression line for all groups. The horizontal line is the median value, the box captures the central 50% of the data (interquartile range), the whiskers include data within 1.5 × of the interquartile range, and outliers are indicated by filled circles. Abbreviations: Cer: *Cercocebus*, Man: *Mandrillus*, Lop: *Lophocebus*, The: *Theropithecus*, Pap: *Papio*, syl: *sylvanus* group of *Macaca*, sil: *silenus* group of *Macaca*, sin: *sinica* group of *Macaca*, fas: *fascicularis* group of *Macaca*, sul: Sulawesi macaques. *p* values with a significance code: ** < 0.001

Table 6 Differences of centroid size (CS) between each group

	Cer	Man	Lop	The	Pap	syl	sil	sin	fas	sul
Cercocebus		0.0000**	0.0365	0.0000**	0.0000**	0.9979	0.0458	0.5611	1.0000	0.0227
Mandrillus	6.8623		0.0000**	0.2603	0.9695	0.0181	0.0000**	0.0000**	0.0000**	0.0000**
Lophocebus	3.2657	6.5354		0.0000**	0.0000**	0.4516	0.0002**	0.0100	0.2657	0.0000**
Theropithecus	6.0828	2.5146	5.8481		0.0449	0.0318	0.0006**	0.0000**	0.0000**	0.0000**
Papio	7.4498	1.2196	7.0403	3.1994		0.0065	0.0000**	0.0000**	0.0000**	0.0000**
Macaca (*sylvanus* gr.)	0.8412	3.4785	2.2073	3.3087	3.7619		0.9923	1.0000	0.9989	0.9958
Macaca (*silenus* gr.)	3.1929	4.9532	4.5976	4.3478	6.0410	1.0000		0.8198	0.0549	0.9991
Macaca (*sinica* gr.)	2.0530	5.8905	3.6469	5.4633	7.0324	0.1946	1.6565		0.5297	0.9996
Macaca (*fascicularis* gr.)	0.2765	6.5707	2.5047	5.8434	7.2054	0.7785	3.1324	2.0968		0.0457
Macaca (Sulawesi)	3.4123	6.1368	5.3481	5.4847	7.2202	0.9234	0.7586	0.6917	3.1934	

Cer: *Cercocebus*, Man: *Mandrillus*, Lop: *Lophocebus,* The: *Theropithecus*, Pap: *Papio*, syl: *sylvanus* group of *Macaca*, sil: silenus group of *Macaca*, sin: *sinica* group of *Macaca*, fas: *fascicularis* group of *Macaca*, sul: Sulawesi macaques

Lower left *t* values, upper right *p* values with a significance code** < 0.001; * < 0.01

score was significantly different between the two genera of the large-bodied forms (*Mandrillus* and *Papio*) and between the two genera of the small-bodied forms (*Cercocebus* and *Lophocebus*) (Table 9, Fig. 5). Regardless of their close phyletic relationships, *Mandrillus* had significantly lower scores than did *Cercocebus*, and *Papio* had significantly higher scores than did *Lophocebus* (Table 9, Fig. 5). Figure 6 and Online Resource 2 depict the principal pattern provided by PC2. Lower scores are characterized by a horizontal dental arch with a long nasal roof and a vertical nasal aperture (i.e., a klinorhynch face), a rounded orbit with a round supraorbital ridge, and a shrunken and anteriorly convex zygomaxillary region; higher scores are characterized by a dorsal flexion of the dental arch with a short nasal roof and a sloping nasal aperture (i.e., an airorhynch face), a sub-rectangular orbit with a horizontal supraorbital ridge, and an expanded and flat zygomaxillary region.

The third principal component (PC3) summarized 8.1% of the total variation (Table 4). The PC3 score was significantly correlated with logCS; however, this correlation

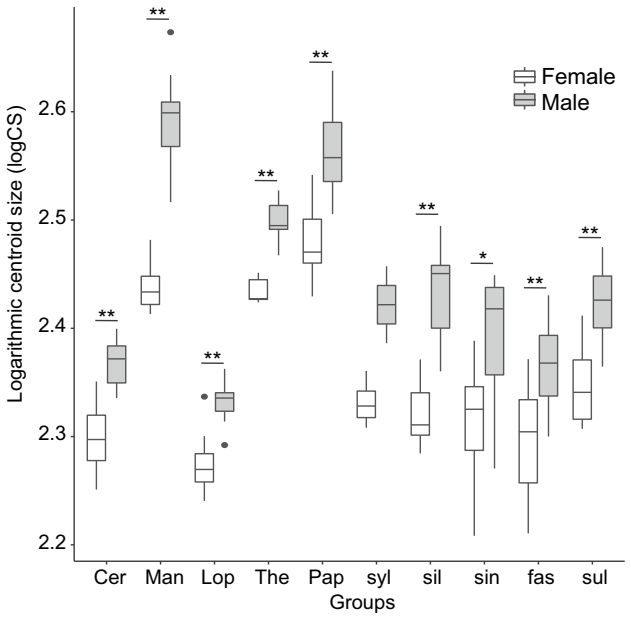

Fig. 3 Box plots of the natural logarithmic centroid size. See Fig. 2 for explanations of the box plot and for the definitions of the abbreviations. *p* values with a significance code: ** < 0.001; * < 0.01

was not strong ($P < 0.001$, $r^2 = 0.0624$; Table 5, Fig. 7a). The differences between sexes were nonsignificant in all groups, excluding *Cercocebus* and the *sinica* group (Table 8, Fig. 7b). The small-bodied African papionins (*Lophocebus* and *Cercocebus*) had high scores, *Theropithecus* and *Mandrillus* of the large-bodied African papionins had low scores, and moderate-bodied macaques (*Macaca*), excluding Sulawesi macaques, had intermediate scores relative to them (Fig. 7). Sulawesi macaques were significantly different from the other papionins, with the exception of the *sylvanus* group (Table 10, Fig. 7). *Papio* was significantly different from the other two genera of the large-bodied African papionins and from *Cercocebus*, and exhibited scores that were comparable to those of non-Sulawesi macaques (Table 10, Fig. 7). Some specimens of *Papio* exhibited scores lower than those of the *sylvanus* group (Fig. 7). Figure 8 and Online Resource 3 depict the principal pattern provided by PC3. Lower scores are characterized by a well developed anteorbital drop with a short and subvertical upper face and orbital aperture, a long muzzle, and a narrow nasal aperture; and higher scores are characterized by a subvertical and smoothly curved sagittal profile with a tall upper face and orbital aperture, a short muzzle, and an ellipsoidal nasal aperture.

The fourth principal component (PC4) summarized 3.1% of the total variation (Table 4). The PC4 score was not significantly correlated with logCS ($P = 0.2189$, $r^2 = 0.0053$; Table 5, Fig. 9a). Sexual differences were significant in half of the groups (Table 8, Fig. 9b). Non-Sulawesi macaques had high scores (Fig. 9). Each species group, with the exception of the *sylvanus* group, usually exhibited a significantly higher score than did African papionins, with the exception of *Mandrillus* (Table 11). The female subjects of the *sylvanus* group had higher scores and the male ones had intermediate scores (Fig. 9); however, a significant difference was not detected between this group and most of the African papionins (Table 11). Sulawesi macaques were smaller and exhibited scores that were comparable to those of the African papionins (Fig. 9). They were significantly different from the *silenus* and *sinica* groups, but were not significantly different from *Papio* and *Cercocebus* (Table 11). *Lophocebus* and *Theropithecus* had low scores (Fig. 9). *Lophocebus* was significantly different in score from the other papionins, with the exception of *Theropithecus*, and *Theropithecus* was significantly different in score from the other papionins, with the exception of *Cercocebus* and *Lophocebus* (Table 11). Figure 10 and Online Resource 4 depict the principal pattern

Table 7 Differences of PC1 scores between groups

	Cer	Man	Lop	The	Pap	syl	sil	sin	fas	sul
Cercocebus		0.0000**	0.1846	0.0000**	0.0000**	0.9962	0.0003**	0.0036*	0.5948	0.0000**
Mandrillus	6.8623		0.0000**	0.1529	1.0000	0.0057*	0.0000**	0.0000**	0.0000**	0.0000**
Lophocebus	2.6731	6.5354		0.0000**	0.0000**	0.4813	0.0000**	0.0000**	0.0005**	0.0000**
Theropithecus	6.0828	2.7531	5.8481		0.0003**	0.0107	0.0000**	0.0000**	0.0000**	0.0009**
Papio	7.4498	0.2076	7.0403	4.4859		0.0038*	0.0000**	0.0000**	0.0000**	0.0000**
Macaca (*sylvanus* gr.)	0.9113	3.7947	2.1648	3.6268	3.8987		0.5633	0.8854	1.0000	0.0155
Macaca (*silenus* gr.)	4.4987	6.0757	5.5104	5.2008	6.5186	2.0500		0.8663	0.0549	0.0215
Macaca (*sinica* gr.)	3.9179	6.6865	5.6149	5.8434	7.2054	1.5181	1.5623		0.6484	0.0000**
Macaca (*fascicularis* gr.)	2.0060	6.6865	4.4039	5.9384	7.2169	0.3114	3.1324	1.9301		0.0000**
Macaca (Sulawesi)	6.9200	5.9163	6.8179	4.2490	6.8462	3.5225	3.4279	5.3954	6.1793	

Cer: *Cercocebus*, Man: *Mandrillus*, Lop: *Lophocebus,* The: *Theropithecus*, Pap: *Papio*, syl: *sylvanus* group of *Macaca*, sil: silenus group of *Macaca*, sin: *sinica* group of *Macaca*, fas: *fascicularis* group of *Macaca*, sul: Sulawesi macaques

Lower left *t* values, upper right *p* values with significance codes **<0.001, *<0.01

Table 8 Differences of centroid size (CS) and PC scores between sexes

	CS	PC1	PC2	PC3	PC4	PC5
Cercocebus	0.0000**	0.0004**	0.2087	0.0014*	0.0003**	0.0054**
Mandrillus	0.0000**	0.0001**	0.5950	0.0215	0.0008**	0.0000**
Lophocebus	0.0000**	0.0002**	0.3669	0.0814	0.3046	0.0007**
Theropithecus	0.0002**	0.0258	0.9644	0.2566	0.0072*	0.0012**
Papio	0.0000**	0.0007**	0.0636	0.0514	0.0478	0.0000**
Macaca (*sylvanus* gr.)	–	–	–	–	–	–
Macaca (*silenus* gr.)	0.0000**	0.0004**	0.8897	0.1356	0.0065*	0.0000**
Macaca (*sinica* gr.)	0.0021*	0.0018*	0.1232	0.0013*	0.1908	0.0000**
Macaca (*fascicularis* gr.)	0.0001**	0.0028*	0.1017	0.0168	0.0122	0.0000**
Macaca (Sulawesi)	0.0000**	0.0066*	0.8923	0.3261	0.0006**	0.0007**

p values with significance codes **< 0.001; *< 0.01

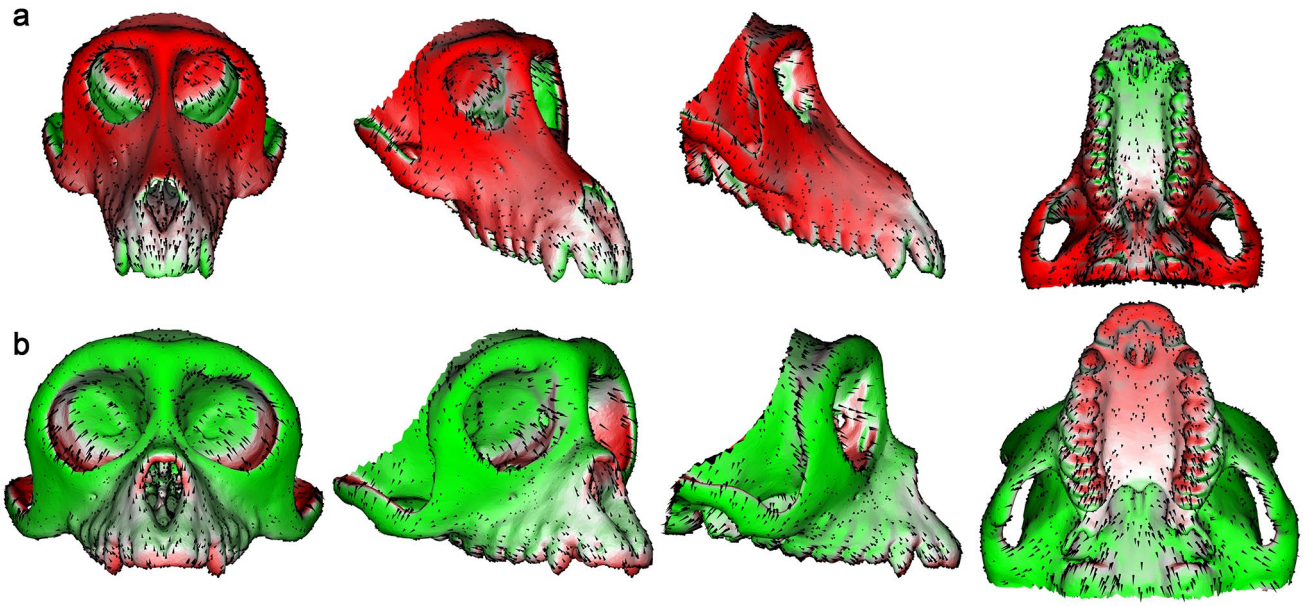

Fig. 4 A depiction of the variation pattern that is summarized by PC1. **a** Higher scores, **b** lower scores. The colors indicate the direction and magnitude of shape changes perpendicular to the surface (green, outward; red, inward), and the arrows indicate shape changes parallel to the surface

provided by PC4. Lower scores are characterized by a narrow upper and middle face with a narrow orbit and nasal aperture, a wide lower face and long premaxilla, and a shallow palate, whereas higher scores are characterized by a proportionally wide upper and middle face with a laterally positioned zygomaxillary region and a laterally positioned lateral rim of the orbital aperture, thus generating a wide orbit, a proportionally narrow lower face and short premaxilla, and a deep palate.

The fifth principal component (PC5) summarized 2.7% of the total variation (Table 4). The PC5 score was not significantly correlated with logCS ($P = 0.0372$, $r^2 = 0.0152$; Table 5, Fig. 11a). Sexual differences were significant in each group, with the exception of the *sylvanus* group (Table 7, Fig. 11b). This means that this principal pattern represented a sexual difference in shape that is common to papionins. *Mandrillus* had intermediate scores that were not significantly different from those of any other papionins (Table 12, Fig. 11). Macaques had high scores (Fig. 11). The *sylvanus* group had scores that were comparable to those of African papionins, whereas the other groups of macaques usually had significantly higher scores than did the African papionins, with the exception of *Mandrillus* (Table 12, Fig. 11). *Theropithecus* had low scores (Fig. 11).

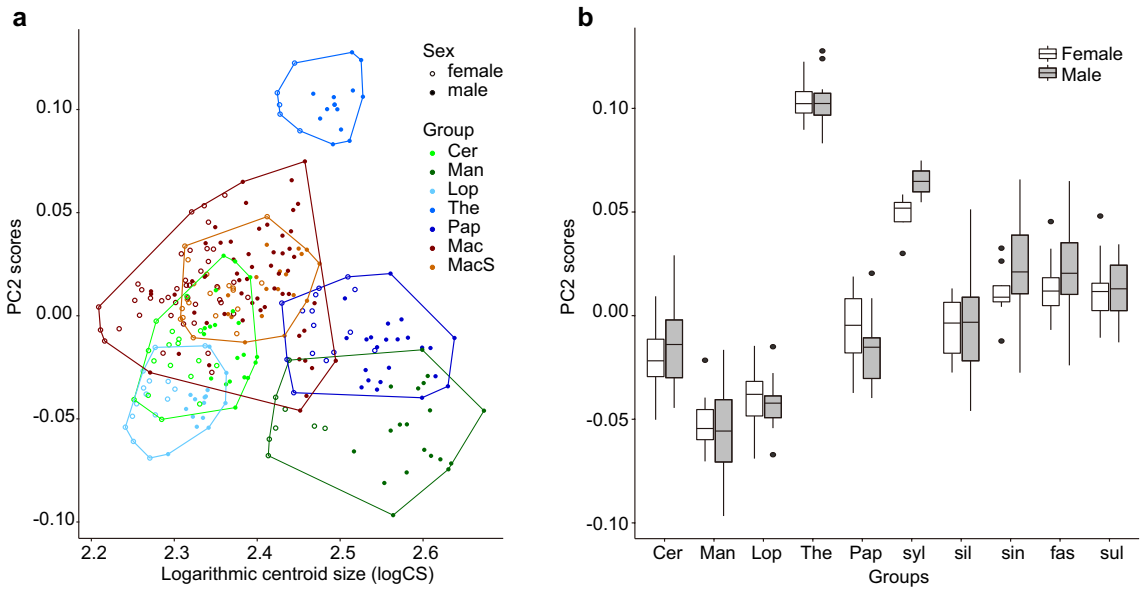

Fig. 5 Scatter (**a**) and box (**b**) plots of PC2 scores. See Fig. 2 for explanations of the box plot and for the definitions of the abbreviations

Table 9 Differences of PC2 scores between groups

	Cer	Man	Lop	The	Pap	syl	sil	sin	fas	sul
Cercocebus		0.0000**	0.0000**	0.0000**	0.9962	0.0040*	0.4448	0.0000**	0.0000**	0.0000**
Mandrillus	5.9349		0.0906	0.0000**	0.0000**	0.0057*	0.0000**	0.0000**	0.0000**	0.0000**
Lophocebus	5.0940	2.9565		0.0000**	0.0000**	0.0052*	0.0000**	0.0000**	0.0000**	0.0000**
Theropithecus	6.0828	5.7663	5.8481		0.0000**	0.0107	0.0000**	0.0000**	0.0000**	0.0000**
Papio	0.9114	6.2925	5.8916	6.1110		0.0038*	0.9022	0.0000**	0.0000**	0.0000**
Macaca (*sylvanus* gr.)	3.8905	3.7947	3.8203	3.6268	3.8987		0.0099*	0.0360	0.0281	0.0074**
Macaca (*silenus* gr.)	2.2171	5.7728	5.4259	5.6273	1.4751	3.6500		0.0051**	0.0038**	0.0298
Macaca (*sinica* gr.)	5.5709	6.6431	6.7159	5.9574	5.4184	3.2697	3.8233		1.0000	0.9671
Macaca (*fascicularis* gr.)	5.7003	6.6576	6.7709	5.9574	5.7182	3.3475	3.9018	0.1090		0.9020
Macaca (Sulawesi)	5.7119	6.9023	7.0403	6.1110	5.5787	3.7277	3.3296	1.2336	1.4757	

Cer: *Cercocebus*, Man: *Mandrillus*, Lop: *Lophocebus,* The: *Theropithecus*, Pap: *Papio*, syl: *sylvanus* group of *Macaca*, sil: silenus group of *Macaca*, sin: *sinica* group of *Macaca*, fas: *fascicularis* group of *Macaca*, sul: Sulawesi macaques

Lower left *t* values; upper right *p* values with significance codes $^{**}<0.001$, $^{*}<0.01$

It had scores that were significantly different from those of the other papionins, with the exception of *Mandrillus* (Table 12). Figure 12 and Online Resource 5 depict the principal pattern provided by PC5. Lower scores are characterized by a reduced canine root region; a laterally-facing zygomaxillary region and a laterally facing lateral rim of the orbit, thus generating a narrow face in frontal view, as well as a small zygomatic arch and temporal fossa; and higher scores are characterized by an expanded canine root region, an anterior-facing zygomaxillary region and an anteriorly facing lateral rim of the orbit, thus generating a wide face in frontal view, and an anteriorly enlarged zygomatic arch and temporal fossa.

Discussion

Macaques have a moderately long and rounded muzzle (Fleagle 2013; Jablonski 2002; Szalay and Delson 1979), a sagittal profile that is smooth and linear or slightly concave without a developed anteorbital drop (Szalay and Delson 1979), and a deep anterior palate (Gilbert et al. 2009), and they lack maxillary and suborbital fossae (Delson 1980; Fleagle 2013; Gilbert et al. 2009; Jablonski 2002; Szalay and Delson 1979), which distinguishes them from the African papionins. The present study confirmed a major and well-known allometric trend that is common to this tribe,

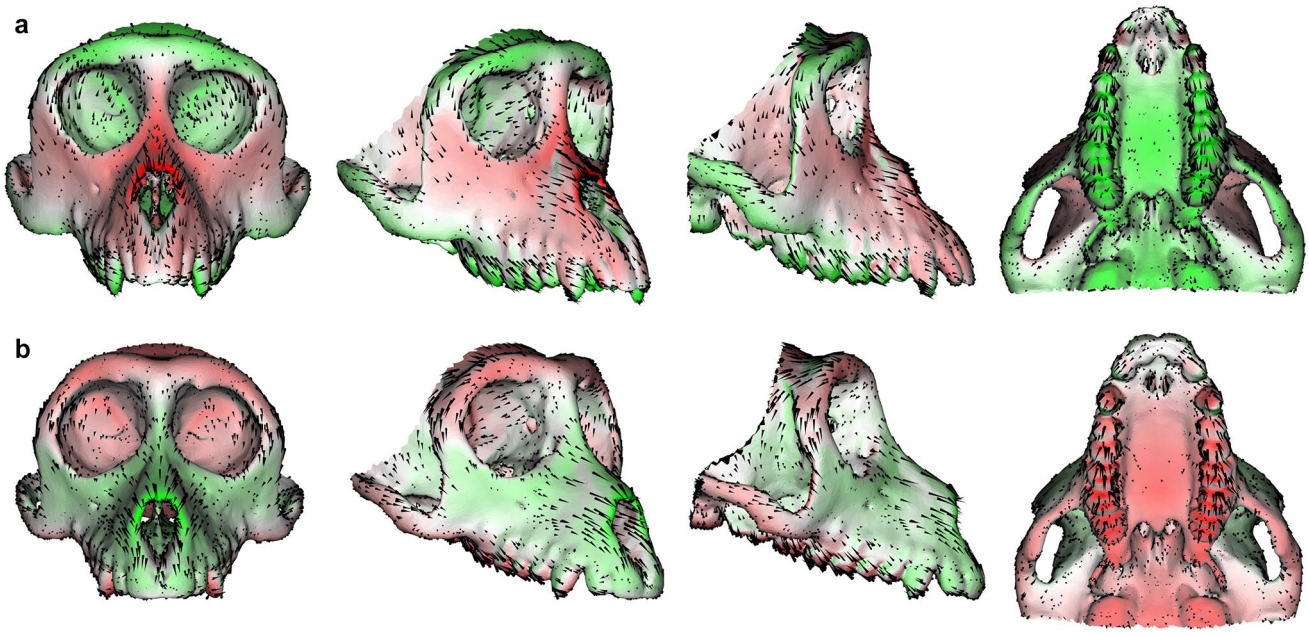

Fig. 6 A depiction of the variation pattern that is summarized by PC2. **a** Higher scores, **b** lower scores. The colors indicate the direction and magnitude of shape changes perpendicular to the surface (green, outward; red, inward), and the arrows indicate shape changes parallel to the surface

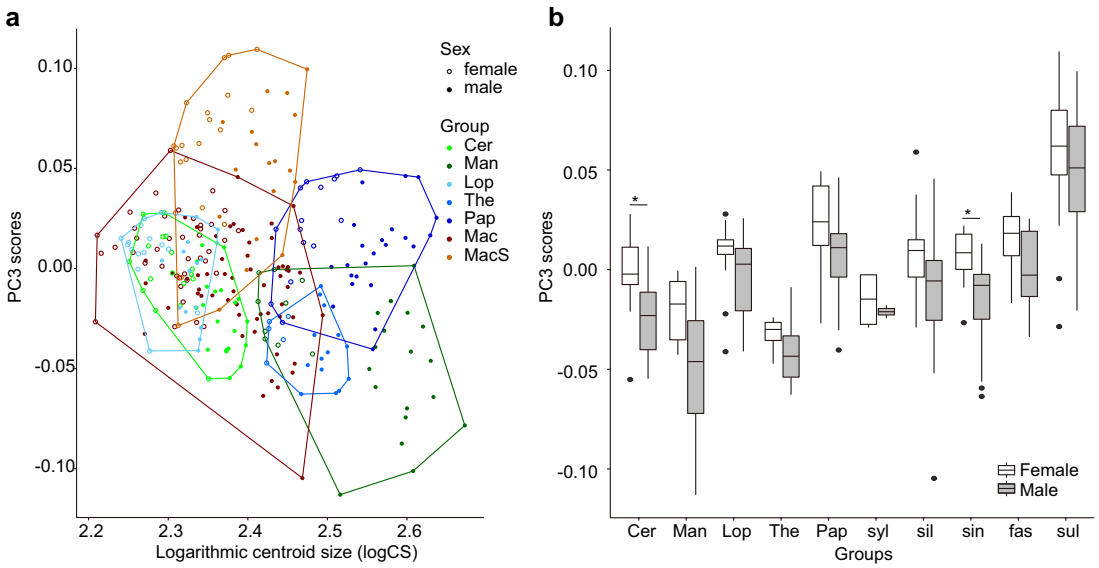

Fig. 7 Scatter (**a**) and box (**b**) plots of PC3 scores. See Fig. 2 for explanations of the box plot and for the definitions of the abbreviations. *p* values with a significance code: * < 0.01

as shown by PC1: large-bodied papionins exhibited a proportionally low, long, and narrow face. This trend has been confirmed in other nonhuman primates, as well as in papionins (Freedman 1962; Frost et al. 2003; Gilbert and Grine 2010; Ito et al. 2011; 2014; Leigh et al. 2003; Shea 1983; Singleton 2002; 2004). A similar trend has been detected in the growth trajectory, i.e., ontogenetic allometry, of nonhuman primates (Collard and O'Higgins 2001; Corner and Richtsmeier 1991; 1992; Mitteroecker et al. 2004; Mouri 1994; O'Higgins and Collard 2002; O'Higgins and Jones 1998; Penin et al. 2002; Shea 1983; Singleton 2012). Thus, this principal pattern explains that the moderately long and rounded muzzle is formed in macaques as a result of their being small-to-moderate-bodied papionins.

Table 10 Differences of PC3 scores between groups

	Cer	Man	Lop	The	Pap	syl	sil	sin	fas	sul
Cercocebus		0.0117	0.1900	0.0040**	0.0006**	0.9999	0.8555	0.9927	0.0044*	0.0000**
Mandrillus	3.6034		0.0000**	1.0000	0.0000**	0.7593	0.0044*	0.0019*	0.0000**	0.0000**
Lophocebus	2.6605	5.0883		0.0000**	0.5984	0.3940	0.9992	0.4649	0.9082	0.0000**
Theropithecus	3.8850	0.2601	4.9247		0.0000**	0.2133	0.0022	0.0008**	0.0000**	0.0000**
Papio	4.3554	5.9682	2.0009	5.6709		0.1348	0.4527	0.0093**	0.9988	0.0000**
Macaca (*sylvanus* gr.)	0.5958	1.7618	2.2922	2.6088	2.8043		0.8718	0.9485	0.1110	0.0138
Macaca (*silenus* gr.)	1.5857	3.8664	0.7437	4.0398	2.2057	1.5500		0.9973	0.8198	0.0000**
Macaca (*sinica* gr.)	0.9942	4.0669	2.1882	4.2661	3.6661	1.3234	0.8714		0.0504	0.0000**
Macaca (*fascicularis* gr.)	3.8649	5.8905	1.4588	5.5583	0.7839	2.8804	1.6565	3.1612		0.0000**
Macaca (Sulawesi)	6.4537	6.6039	5.5334	5.9756	5.1424	3.5567	5.1700	6.1447	5.3147	

Cer: *Cercocebus*, Man: *Mandrillus*, Lop: *Lophocebus,* The: *Theropithecus*, Pap: *Papio*, syl: *sylvanus* group of *Macaca*, sil: silenus group of *Macaca*, sin: *sinica* group of *Macaca*, fas: *fascicularis* group of *Macaca*, sul: Sulawesi macaques

Lower left *t* values, upper right *p* values with significance codes $^{**}<0.001$, $^{*}<0.01$

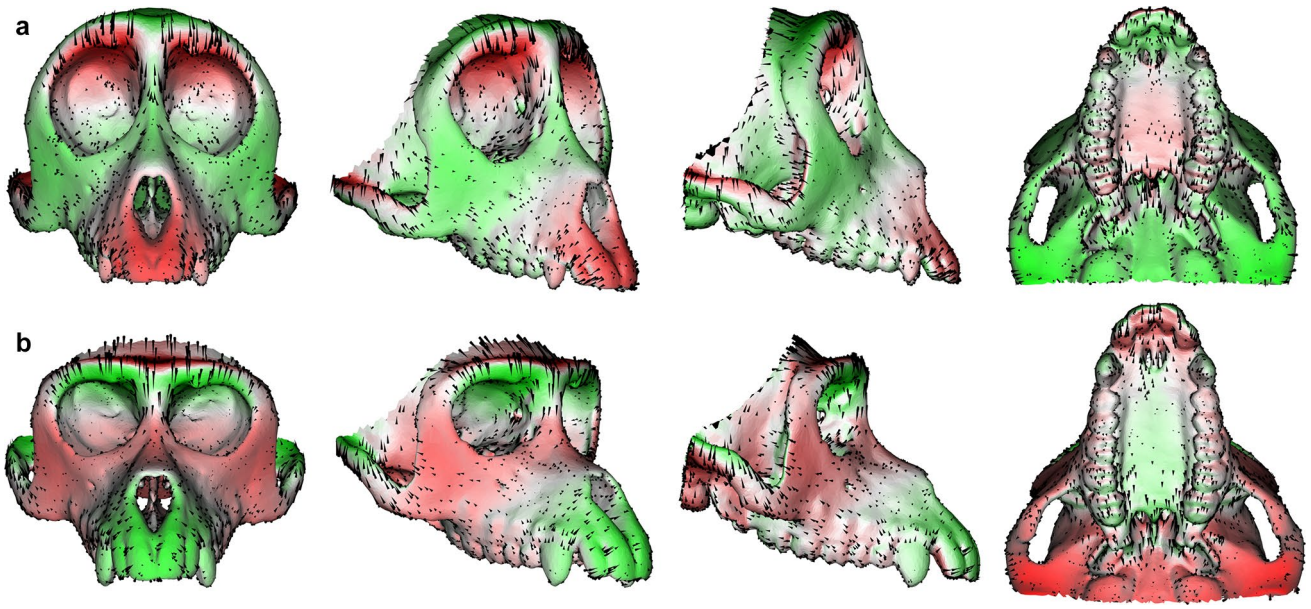

Fig. 8 A depiction of the variation pattern that is summarized by PC3. **a** Higher scores, **b** lower scores. The colors indicate the direction and magnitude of shape changes perpendicular to the surface (green, outward; red, inward), and the arrows indicate shape changes parallel to the surface

Macaques possess many distinct features in facial shape that are apparently not greatly influenced by size and allometric effects, as summarized here in the principal patterns of PC2 to PC5. Every macaque species group exhibited varied combinations of the principal patterns that were different from African papionins. There was a gradient in the variation of PC2, PC4, and PC5 from macaques to African papionins. The *sinica* and *fascicularis* groups shared the features of all three patterns that were different from those of African papionins, with the exception of PC4 and PC5 of *Mandrillus*. The *silenus* group also shared the features of PC4 and PC5, while this group possessed features of PC2 that were comparable to those observed in *Papio* and *Cercocebus*. The two latter African papionins also exhibited features that were close to those of macaques compared with the other African papionins. In contrast, the *sylvanus* group shared features only in PC2 with the *sinica* and *fascicularis* groups and this group showed features in PC4 and PC5 that were not significantly different from those of African papionins. The *sylvanus* group exhibited a separation of the range in the PC4 scores between males and females, although there were not statistically significant sexual differences. The scores

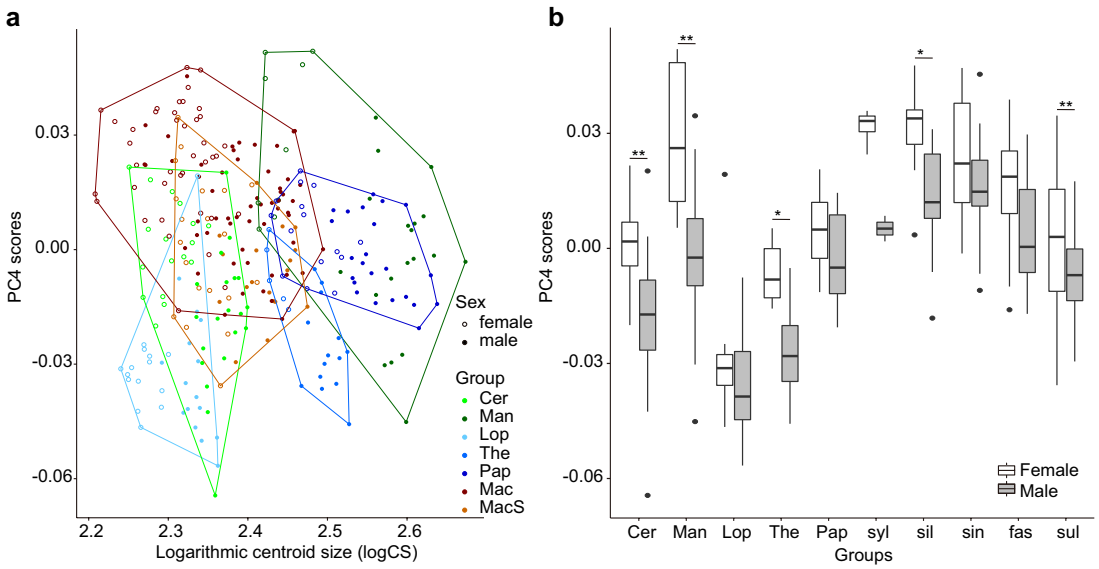

Fig. 9 Scatter (**a**) and box (**b**) plots of PC4 scores. See Fig. 2 for explanations of the box plot and for the definitions of the abbreviations. *p* values with a significance code: ** < 0.001; * < 0.01

Table 11 Differences of PC4 scores between groups

	Cer	Man	Lop	The	Pap	syl	sil	sin	fas	sul
Cercocebus		0.0817	0.0000**	0.2320	0.2294	0.0265	0.0000**	0.0000**	0.0008**	0.8683
Mandrillus	2.9940		0.0000**	0.0017*	0.9055	0.8963	0.5002	0.3599	1.0000	0.6462
Lophocebus	5.1066	5.3840		0.1541	0.0000**	0.0072*	0.0000**	0.0000**	0.0000**	0.0000**
Theropithecus	2.5698	4.0971	2.7496		0.0002**	0.0135	0.0000**	0.0000**	0.0000**	0.0091*
Papio	2.5751	1.4661	6.4350	4.5537		0.1132	0.0004**	0.0000**	0.1888	0.9953
Macaca (*sylvanus* gr.)	3.3648	1.4908	3.7354	3.5632	2.8727		0.9999	0.9999	0.6371	0.0861
Macaca (*silenus* gr.)	5.2162	2.1381	6.1020	5.3193	4.4394	0.5500		1.0000	0.4855	0.0003**
Macaca (*sinica* gr.)	5.8062	2.3446	6.5645	5.7484	5.0841	0.5449	0.2120		0.5757	0.0000**
Macaca (*fascicularis* gr.)	4.2649	0.5066	6.4269	5.0643	2.6631	1.9462	2.1589	2.0327		0.0666
Macaca (Sulawesi)	1.5578	1.9332	6.0027	3.6734	0.9350	2.9753	4.5237	4.9112	3.0666	

Cer: *Cercocebus*, Man: *Mandrillus*, Lop: *Lophocebus,* The: *Theropithecus*, Pap: *Papio*, syl: *sylvanus* group of *Macaca*, sil: silenus group of *Macaca*, sin: *sinica* group of *Macaca*, fas: *fascicularis* group of *Macaca*, sul: Sulawesi macaques

Lower left *t* values, upper right *p* values with significance codes ** < 0.001; * < 0.01

of PC4 in male and PC5 in female ranged within those in African papionins and this finding in part accounts for these statistically significant results. This group comprises only *Macaca sylvanus*, and thus a small sample of this group was used for this study, while future studies are expected to use a larger sample from this group to examine these features. Sulawesi macaques also shared features only in PC2 with the *sinica* and *fascicularis* groups, but they had a distinct facial shape in PC3 that was significantly different from that of both African papionins and non-Sulawesi macaques. Thus, the present study showed that there was a gradient in the shape variations from macaques to African papionins, and the *fascicularis* and *sinica* groups exhibited a contrasting shape against African papionins compared with the other species groups of macaques, but macaques simultaneously showed a large intrageneric variation in every feature, which precluded the separation of all macaques from African papionins using any single feature.

Singleton (2002) applied a method similar to that reported here to detect the principal patterns among African papionins, using a sample of *Macaca fascicularis* as an outgroup. Although that study cannot be compared directly with the present study because of its research aim and design, which were different from ours, Singleton (2002) also describes some of the patterns that were detected here for the *fascicularis* group: variation from the "airorhynch"

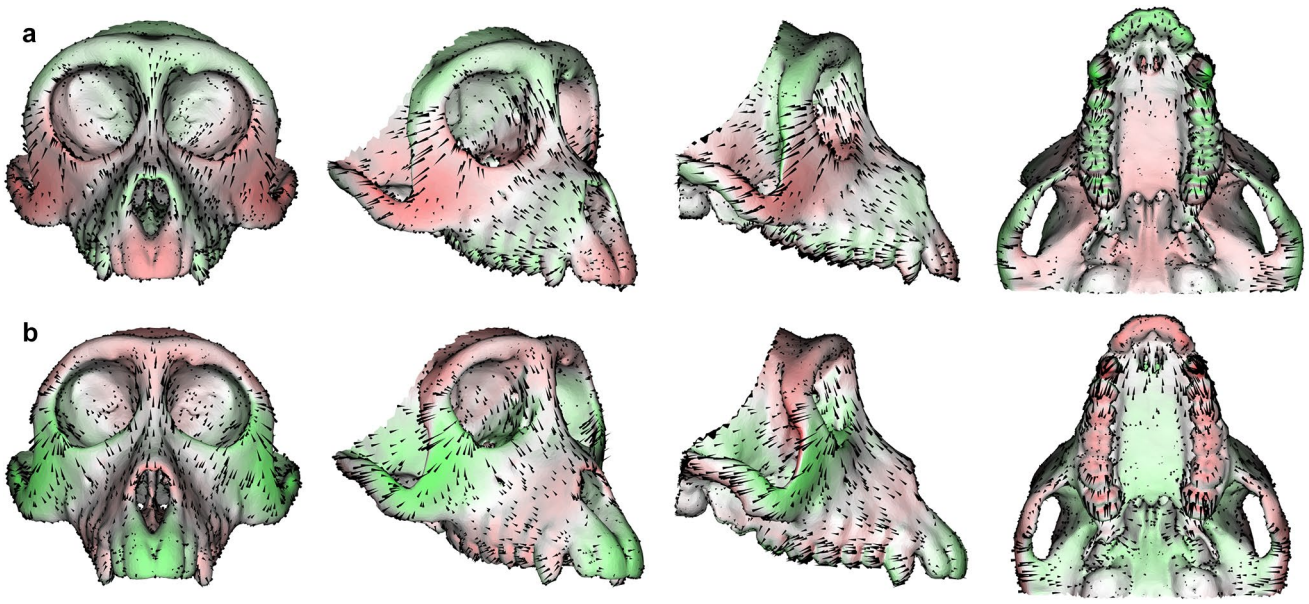

Fig. 10 A depiction of the variation pattern that is summarized by PC4. **a** Higher scores, **b** lower scores. The colors indicate the direction and magnitude of shape changes perpendicular to the surface (green, outward; red, inward), and the arrows indicate shape changes parallel to the surface

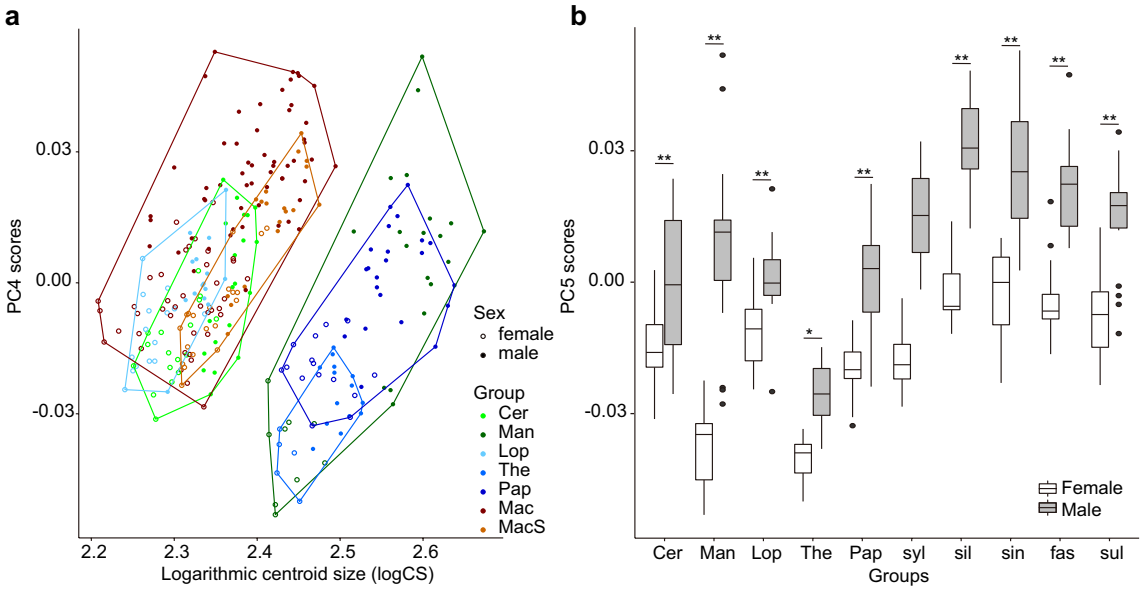

Fig. 11 Scatter (**a**) and box (**b**) plots of PC5 scores. See Fig. 2 for explanations of the box plot and for the definitions of the abbreviations. *p* values with a significance code: ** < 0.001; * < 0.01

to the "klinorhynch" face based on its PC2, and variation in the orbital and zygomaxillary region based on its PC4. The variations summarized by those two PCs correspond almost completely to those provided by the PC2 and PC4 in the present study, respectively. Singleton (2002) also reported a similarity between *M. fascicularis* and *Papio* in the former pattern and between *M. fascicularis* and female *Mandrillus* in the latter pattern. Such similarities were also confirmed by the present study. Thus, the present study used a larger sample including every species group of macaques to provide a better understanding of the distinctions and similarities in facial shape between the two subtribes.

This study showed that macaques, especially the *sylvanus* group, possessed an airorhynch face compared with African

Table 12 Differences of PC5 scores between groups

	Cer	Man	Lop	The	Pap	syl	sil	sin	fas	sul
Cercocebus		1.0000	0.9976	0.0000**	1.0000	1.0000	0.0001**	0.0001**	0.0033*	0.1335
Mandrillus	0.1060		1.0000	0.2720	1.0000	1.0000	0.0263	0.0491	0.4567	0.8176
Lophocebus	0.8574	0.1712		0.0000**	0.9998	0.9990	0.0010*	0.0001**	0.0540	0.7093
Theropithecus	5.1137	2.4929	5.3146		0.0000**	0.1849	0.0000**	0.0000**	0.0000**	0.0000**
Papio	0.0000	0.0649	0.6423	4.9261		1.0000	0.0001**	0.0001**	0.0035*	0.1647
Macaca (*sylvanus* gr.)	0.3154	0.0000	0.7641	2.6724	0.3078		0.3888	0.3658	0.7886	0.9540
Macaca (*silenus* gr.)	4.7139	3.3675	4.2258	5.6273	4.6923	2.3000		0.9992	0.4095	0.0407
Macaca (*sinica* gr.)	4.6885	3.1696	4.6929	5.8244	4.7728	2.3355	0.7458		0.8999	0.1744
Macaca (*fascicularis* gr.)	3.9355	2.1999	3.1377	5.9004	3.9197	1.7127	2.2688	1.4812		0.9256
Macaca (Sulawesi)	2.8083	1.6607	1.8403	5.8740	2.7218	1.2996	3.2312	2.6977	1.4065	

Cer: *Cercocebus*, Man: *Mandrillus*, Lop: *Lophocebus,* The: *Theropithecus*, Pap: *Papio*, syl: *sylvanus* group of *Macaca*, sil: silenus group of *Macaca*, sin: *sinica* group of *Macaca*, fas: *fascicularis* group of *Macaca*, sul: Sulawesi macaques

Lower left *t* values, upper right, *p* values with significance codes** < 0.001; * < 0.01

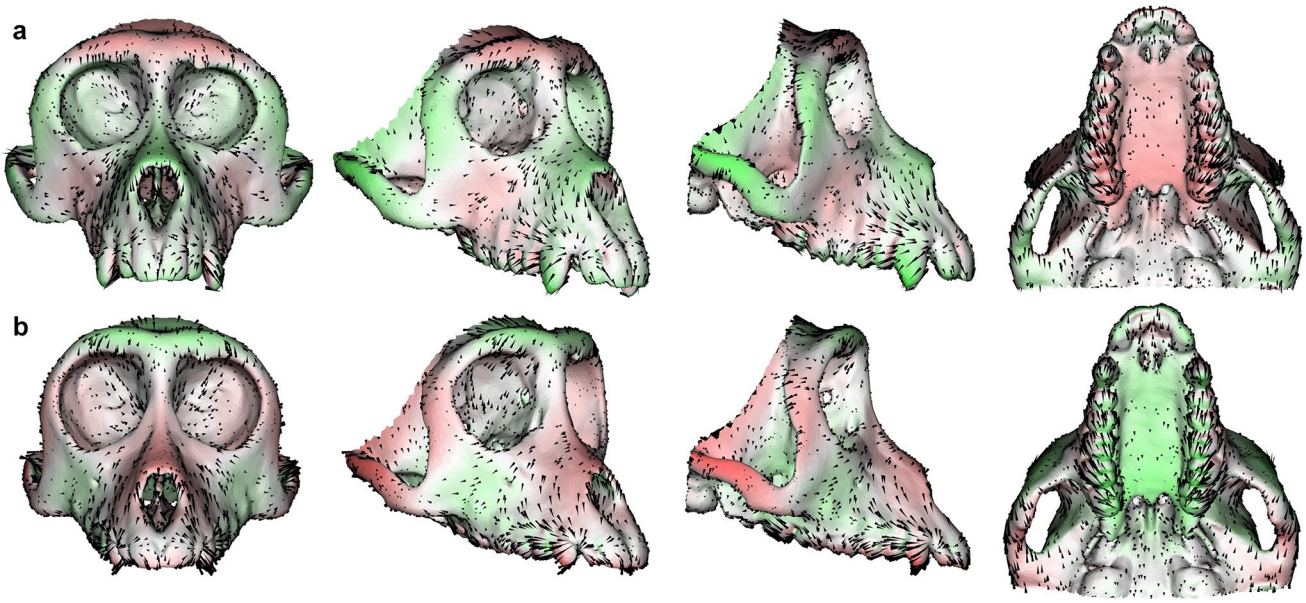

Fig. 12 A depiction of the variation pattern that is summarized by PC5. **a** Higher scores, **b** lower scores. The colors indicate the direction and magnitude of shape changes perpendicular to the surface (green, outward; red, inward), and the arrows indicate shape changes parallel to the surface

papionins, other than *Theropithecus* with its highly airorhynch face, as shown by PC2. While this variation from an airorhynch to a klinorhynch face was suggested to be one of the features that might be affected by the ontogenetic allometric effect in baboons (Leigh 2006), its detection can be precluded by the variation in facial length caused by a major allometric trend. This study confirmed that this variation was extracted independently with the other principal patterns, including the major evolutionary allometric effect, as one of the important features that differentiate macaques from African papionins. A decrease of cranial base flexion increases relative neurocranial volume, resulting in an airorhynch face in haplorhines compared with strepsirrhines (Lieberman et al. 2000; Ross and Ravosa 1993). Those differences are limited between macaques/*Theropithecus* and the other African papionins (Lieberman et al. 2000; Ross and Ravosa 1993), but future studies are expected to examine variation in cranial structures to understand the evolutionary diversification in facial kyphosis among macaques, *Theropithecus*, and other African papionins.

This study also provides strong support for the view that a moderately smooth sagittal profile is present in macaques, as shown by PC3. These features, which were inherited by extant macaques, are believed to be an

ancestral and generalized condition for this tribe (Collard and O'Higgins 2001; Delson 1980; Fleagle 2013; Szalay and Delson 1979). We also confirmed that Sulawesi macaques possessed a slightly convex and smooth profile that is distinctive among papionins, as shown by the deviation from the other papionins in PC3. They are unusual in that they transgress Wallace's line, which is a deep-sea barrier to non-volant faunal interchange (Evans et al. 1999; Fooden 1969; Takenaka et al. 1987). Their *nemestrina*-like ancestors likely dispersed to Sulawesi twice in the Pleistocene and remained isolated on this island (Evans et al. 1999; Takenaka et al. 1987). This distinct facial shape observed in Sulawesi macaques was probably formed after geographical isolation from the population of the other members of the *silenus* group. The sagittal profile in these macaques contrast with those of *Mandrillus* and *Theropithecus*. These large-bodied African papionins had a well-developed anteorbital drop made by a subvertical upper face and a long and subhorizontal nasal roof. These features have often been selected to characterize large-bodied African papionins, while they are not distinctive in small-bodied forms (Fleagle 2013; Szalay and Delson 1979). However, the situation observed in *Papio* added confusion to this view; this study showed that *Papio* exhibited a reduced degree of anteorbital drop, resembling that detected in non-Sulawesi macaques. Further, some specimens of *Papio* exhibited a lesser degree of anteorbital drop compared with the *sylvanus* group. The degree of anteorbital drop that can be detected by the naked eye is also affected by a combination of the other principal patterns, including an allometric effect. The "anteorbital drop" in large-bodied African papionins is not well defined, but it may be roughly described as the concavity formed by the subvertical interorbital part of the upper face and the subhorizontal nasal roof (muzzle dorsum) in the midline sagittal profile. The common allometric trend, as shown by PC1, indicated that macaques had a smaller angle between the upper face and the nasal roof. In addition, macaques had an airorhynch face to reduce the angle, as shown by PC2. Nevertheless, it does not form an "anteorbital drop", because they had a short nasal roof. On the other hand, whereas the large-bodied African papionins had a long and klinorhynch face, as shown by PC1 and PC2, they had a long nasal roof. Such a long nasal roof probably makes an "anteorbital drop" easily detectable by the naked eye in large-bodied African papionins including *Papio*. This study showed that the "anteorbital drop" in *Papio* was probably formed by a combination different from that in phylogenetically close *Theropithecus*, as well as in *Mandrillus*. *Papio* is a nonhuman primate that has expanded their geographical distribution, in part sympatric with the other African papionins, and it achieved a successful adaptation in varied habitats and a wide geographical distribution in Africa (Gilbert 2013; Jolly 1967; Williams et al. 2007). Thus, specimens of *Papio* are easily available, and this animal is often regarded as a representative of African large-bodied papionins against macaques in morphological studies. However, caution is needed, for example, when evaluating the phyletic position of Eurasian large papionins from the Plio-Pleistocene.

This study in part explained many distinct morphological features generated by the lesser principal patterns in macaques. The major allometric trend (PC1) also made the nasal aperture vertical and proportionally long in macaques. This means that such a feature is shared by macaques and small-bodied African papionins in part because they are small-to-moderate-bodied papionins. Nevertheless, a sloping nasal aperture generating a long nasal aperture in the frontal and lateral views in macaques was also associated with the airorhynch face in macaques, as shown by PC2. This feature was preserved in macaques independently of the allometric trend. This study also showed the tendency toward a wide upper and middle face and a narrow lower face in macaques, as shown by PC4. Such a feature is formed by a laterally positioned lateral region of the face, including the zygomaxillary region and the lateral rim of the orbit, thus widening the orbit. In addition, macaques generally possessed an anterior-faced zygomaxillary region compared with African papionins. Such a feature generates a flat and wide lateral part of the face in the frontal view in macaques compared with African papionins. These features of a wide face were also preserved independently of the major allometric trend generating a proportionally large upper face and small lower face in macaques. In addition, the palate was deep in macaques compared with African papionins, as shown by PC4. A deep anterior palate is one of the distinct characters of macaques compared with African papionins (Gilbert et al. 2009). Such a distinct feature, which can be detected using the naked eye, was not extracted solely by any principal pattern in this study, but was expected to appear by any effect making the posterior palate shallow via a combination of several patterns. Therefore, many distinct features in macaques are preserved by the lesser principal patterns even after the elimination of the major evolutionary allometric effect.

Lastly, sexual difference in the canine region was common to every group in the two subtribes, as shown by PC5. This difference probably reflects the differences in canine size. The difference in canine size by sex is representative of characters for evaluating a degree of sexual dimorphism in nonhuman primates (Plavcan and van Schaik 1994; Plavcan et al. 1995). This study also showed a sexual difference in the cheek region: an anteriorly-facing zygomaxillary region and an anteriorly enlarged zygomatic arch in males. Such a feature reflects the enlargement of the temporal fossa to accommodate the more developed masseter and temporalis

muscles in males compared with females. It should be noted that the specimens used here did not show a significant sexual difference in PC1 scores in *Theropithecus*. The specimens used here were sampled from both wild and captive sources and from younger to older adult individuals, and they were housed at four different institutions, which means that this finding is not due to specific population or generation. The finding indicates that an allometric effect common to this tribe weakly affects this genus. In addition, *Theropithecus* had a distinctly airorhynch face, as shown by PC2. These findings suggest that a different ontogenetic allometry may be presented by this genus. Future studies are expected to examine developmental changes in facial shape to understand these distinct features in *Theropithecus*.

This study confirmed the major allometric trend that is well known in papionins. Evolutionary modifications in size potentially occurred because of environmental and climatic fluctuations in the habitats of a given animal, e.g., through physical adaptation in terms of thermoregulation (Fooden and Albrecht 1993; Ito et al. 2014). This means that a large-bodied macaque would have possessed a low, long, and narrow face, which are features that are comparable to those of the extant large-bodied African papionins. The landmark data used here were limited to a direct extraction of the distinctive characters that are known in papionins, e.g., a maxillary fossa in the large-bodied African papionins, a suborbital hollow in the small-bodied African papionins, and bilateral protruding ridges of the muzzle in *Mandrillus*. Alternatively, this study extracted features in facial distortion that were different between macaques and African papionins after the elimination of the allometric effect on the facial shape: macaques usually possessed an airorhynch face, a moderately smooth profile, and a lateral-positioned, anterior-facing, wide cheek region including the zygomaxillary region and the lateral rim of the orbit. Nevertheless, it should be noted that these features are not always easily detected by the naked eye. The major allometric effect (PC1) accounted for a large amount of the total variation (57.8%); therefore, it sometimes hid and precluded the detection of the features summarized by the other less-principal patterns in the real world. These lesser variations thus become the subject in evaluating the shape differences between the two subtribes after appropriate adjustments to eliminate or reduce the allometric effects over the shape features. The entire face is rarely preserved, and the landmark data used here are not available in many cases of fossil specimens. Therefore, although different landmark data sets need to be customized for specific studies, the information provided by this study is expected to improve the customization and phyletic comparisons of the fossil papionins without disturbances from the potential evolutionary fluctuation in the size of a given specimen.

Acknowledgements We express our gratitude to L. Heaney, W. Stanley, E. M. Langan, D. P. Lunde, and E. Westwig for help with skeletal examinations. We also thank E. Delson and an anonymous reviewer for careful examination of our manuscript and providing useful suggestions. This research was financially supported in part by a JSPS Grant-in-Aid for Scientific Research (Grant 26650171 to T.N), the Keihanshin Consortium for Fostering the Next Generation of Global Leaders in Research (K-CONNEX, to T.I.), and the Cooperative Research Program of the Primate Research Institute of Kyoto University (Grant 2016-A-10 and 2017-A-10 to N.M.).

References

Adams DC, Collyer ML, Kaliontzopoulou A (2019) Geomorph: software for geometric morphometric analyses, R package version 3.1.0. https://cran.r-project.org/package=geomorph

Alba DM, Delson E, Carnevale G, Colombero S, Delfino M, Giuntelli P, Pavia M, Pavia G (2014) First joint record of Mesopithecus and cf. Macaca in the Miocene of Europe. J Hum Evol 67:1–18. https://doi.org/10.1016/j.jhevol.2013.11.001

Alba DM, Delson E, Morales J, Montoya P, Romero G (2018) Macaque remains from the early Pliocene of the Iberian Peninsula. J Hum Evol 123:141–147. https://doi.org/10.1016/j.jhevol.2018.07.005

Albrecht GH (1978) The craniofacial morphology of the Sulawesi macaques: multivariate approaches to biological problems. Contrib Primatol 13:1–151

Belmaker M (2010) The presence of a large cercopithecine (cf. Theropithecus sp.) in the 'Ubeidiya formation (Early Pleistocene, Israel). J Hum Evol 58:79–89. https://doi.org/10.1016/j.jhevol.2009.08.004

Bookstein F (1991) Morphometric tools for landmark data: geometry and biology. Camnridge University Press, Cambridge

Cardini A, Jansson AU, Elton S (2007) A geometric morphometric approach to the study of ecogeographical and clinal variation in vervet monkeys. J Biogeogr 34:1663–1678. https://doi.org/10.1111/j.1365-2699.2007.01731.x

Collard M, O'Higgins P (2001) Ontogeny and homoplasy in the papionin monkey face. Evol Dev 3:322–331. https://doi.org/10.1046/j.1525-142X.2001.01042.x

Collard M, Wood B (2001) Homoplasy and the early hominid masticatory system: inferences from analyses of extant hominoids and papionins. J Hum Evol 41:167–194. https://doi.org/10.1006/jhev.2001.0487

Corner BD, Richtsmeier JT (1991) Morphometric analysis of craniofacial growth in Cebus apella. Am J Phys Anthropol 84:323–342. https://doi.org/10.1002/ajpa.1330840308

Corner BD, Richtsmeier JT (1992) Cranial growth in the squirrel monkey (Saimiri sciureus): a quantitative analysis using three dimensional coordinate data. Am J Phys Anthropol 87:67–81. https://doi.org/10.1002/ajpa.1330870107

Delson E (1980) Fossil macaques, phyletic relationships and a scenario of deployment. In: Lindburg DG (ed) The macaques: studies in ecology, behavior, and evolution. Van Nostrand Reinhold, New York, pp 10–30

Delson E (1993) Theropithecus fossils from Africa and India and the taxonomy of the genus. In: Jablonski NG (ed) Theropithecus: the rise and fall of a primate genus. Cambridge University Press, Cambridge, pp 157–190. https://doi.org/10.1017/cbo9780511565540.006

Delson E (2000) Cercopithecinae. In: Delson E, Tattersall I, Van Couvering JA, Brooks AS (eds) Encyclopedia of human evolution and prehistory. Garland Publishing, New York, pp 166–171

Disotell TR (1994) Generic level relationships of the Papionini (Cercopithecoidea). Am J Phys Anthropol 94:47–57. https://doi.org/10.1002/ajpa.1330940105

TR Disotell (1996) The phylogeny of Old World monkeys. Evol Anthropol 5:18–24. 10.1002/(SICI)1520-6505(1996)5:1<18::AID-EVAN6>3.0.CO;2-S

Disotell TR (2000) Molecular systematics of the Cercopithecidae. In: Whitehead PF, Jolly CJ (eds) Old World monkeys. Cambridge University Press, Cambridge, pp 29–56. https://doi.org/10.1017/cbo9780511542589.003

Evans BJ, Morales JC, Supriatna J, Melnick DJ (1999) Origin of the Sulawesi macaques (Cercopithecidae: macaca) as suggested by mitochondrial DNA phylogeny. Biol J Linn Soc 66:539–560. https://doi.org/10.1006/bijl.1998.0292

Fleagle JG (2013) Primate adaptation and evolution, 3rd edn. Academic Press, Amsterdam

Fooden J (1969) Taxonomy and evolution of monkeys of Celebes (Primates - Cercopithecidae). Bibliotheca Primatologica 10:1–148

Fooden J (1976) Provisional classifications and key to living species of macaques (primates: macaca). Folia Primatol (Basel) 25:225–236. https://doi.org/10.1159/000155715

Fooden J (1980) Classification and distribution of living macaques (Macaca Lacepede, 1799). In: Lindburg DG (ed) The macaques: studies in ecology, behavior, and evolution. Van Nostrand Reinhold, New York, pp 1–9

Fooden J, Albrecht GH (1993) Latitudinal and insular variation of skull size in crab-eating macaques (Primates, Cercopithecidae: macaca fascicularis). Am J Phys Anthropol 92:521–538. https://doi.org/10.1002/ajpa.1330920409

Fox J, Weisberg S (2019) An {R} companion to applied regression, 3rd ed. Sage Publishing, Thousand Oaks. https://socialsciences.mcmaster.ca/jfox/Books/Companion/

Freedman L (1962) Growth of muzzle length relative to calvaria length in Papio. Growth 26:117–128

Frost SR (2001) New Early Pliocene Cercopithecidae (Mammalia: primates) from Aramis, Middle Awash Valley, Ethiopia. Am Mus Novit 3350:1–36

Frost SR, Marcus LF, Bookstein FL, Reddy DP, Delson E (2003) Cranial allometry, phylogeography, and systematics of large-bodied papionins (Primates: cercopithecinae) inferred from geometric morphometric analysis of landmark data. Anat Rec A Discov Mol Cell Evol Biol 275:1048–1072. https://doi.org/10.1002/ar.a.10112

Gibert J, Ribot F, Gibert L, Leakey M, Arribas A, Martinez B (1995) Presence of the cercopithecid genus Theropithecus in Cueva-Victoria (Murcia, Spain). J Hum Evol 28:487–493. https://doi.org/10.1006/jhev.1995.1036

Gilbert CC (2007) Craniomandibular morphology supporting the diphyletic origin of mangabeys and a new genus of the Cercocebus/Mandrillus clade, Procercocebus. J Hum Evol 53:69–102. https://doi.org/10.1016/j.jhevol.2007.03.004

Gilbert CC (2013) Cladistic analysis of extant and fossil African papionins using craniodental data. J Hum Evol 64:399–433. https://doi.org/10.1016/j.jhevol.2013.01.013

Gilbert CC, Grine FE (2010) Morphometric variation in the papionin muzzle and the biochronology of the South African Plio-Pleistocene karst cave deposits. Am J Phys Anthropol 141:418–429. https://doi.org/10.1002/ajpa.21160

Gilbert CC, Rossie JB (2007) Congruence of molecules and morphology using a narrow allometric approach. Proc Natl Acad Sci USA 104:11910–11914. https://doi.org/10.1073/pnas.0702174104

Gilbert CC, Frost SR, Strait DS (2009) Allometry, sexual dimorphism, and phylogeny: a cladistic analysis of extant African papionins using craniodental data. J Hum Evol 57:298–320. https://doi.org/10.1016/j.jhevol.2009.05.013

Gilbert CC, Stanley WT, Olson LE, Davenport TR, Sargis EJ (2011) Morphological systematics of the kipunji (Rungwecebus kipunji) and the ontogenetic development of phylogenetically informative characters in the Papionini. J Hum Evol 60:731–745. https://doi.org/10.1016/j.jhevol.2011.01.005

Gilbert CC, Frost SR, Pugh KD, Anderson M, Delson E (2018) Evolution of the modern baboon (Papio hamadryas): a reassessment of the African Plio-Pleistocene record. J Hum Evol 122:38–69. https://doi.org/10.1016/j.jhevol.2018.04.012

Gupta VJ, Sahni A (1981) Theropithecus delsoni, a new cercopithecine species from the Upper Siwaliks of India. Bulletin of the Indian Geological Association 14:69–71

Harris EE (2000) Molecular systematics of the old world monkey tribe papionini: analysis of the total available genetic sequences. J Hum Evol 38:235–256. https://doi.org/10.1006/jhev.1999.0318

Hothorn T, Hornik K, van de Wiel MA, Zeileis A (2006) A lego system for conditional inference. Am Stat 60(3):257–263

Ito T, Nishimura T, Takai M (2011) Allometry and interspecific differences in the facial cranium of two closely related macaque species. Anatomy research international 2011:849751. https://doi.org/10.1155/2011/849751

Ito T, Nishimura T, Takai M (2014) Ecogeographical and phylogenetic effects on craniofacial variation in macaques. Am J Phys Anthropol 154:27–41. https://doi.org/10.1002/ajpa.22469

Jablonski NG (2002) Fossil old world monkeys: the late Neogene radiation. In: Hartwig WC (ed) The primate fossil records. Cambridge University Press, Cambridge, pp 255–299

Jablonski NG, Frost S (2010) Cercopithecoidea. In: Werdelin L, Sanders WJ (eds) Cenozoic mammals of Africa. University of California Press, Berkeley, pp 393–428

Jolly CJ (1967) The evolution of the baboons. In: Wagtborg H (ed) The baboon in medical research, vol 2. University of Texas Press, Austin, pp 23–50

Kieser JA, Groeneveld HT (1987) Craniodental allometry in the Chacma baboon (Papio ursinus). S Afr J Sci 83:379–379

Kostopoulos DS, Guy F, Kynigopoulou Z, Koufos GD, Valentin X, Merceron G (2018) A 2 Ma old baboon-like monkey from Northern Greece and new evidence to support the Paradolichopithecus—Procynocephalus synonymy (Primates: cercopithecidae). J Hum Evol 121:178–192. https://doi.org/10.1016/j.jhevol.2018.02.012

Leigh SR (2006) Cranial ontogeny of Papio baboons (Papio hamadryas). Am J Phys Anthropol 130:71–84. https://doi.org/10.1002/ajpa.20319

Leigh SR (2007) Homoplasy and the evolution of ontogeny in papionin primates. J Hum Evol 52:536–558. https://doi.org/10.1016/j.jhevol.2006.11.016

Leigh SR, Shah NF, Buchanan LS (2003) Ontogeny and phylogeny in papionin primates. J Hum Evol 45:285–316. https://doi.org/10.1016/j.jhevol.2003.08.004

Li QQ, Zhang YP (2005) Phylogenetic relationships of the macaques (Cercopithecidae: macaca), inferred from mitochondrial DNA sequences. Biochem Genet 43:375–386. https://doi.org/10.1007/s10528-005-6777-z

Li J et al (2009) Phylogeny of the macaques (Cercopithecidae: macaca) based on Alu elements. Gene 448:242–249. https://doi.org/10.1016/j.gene.2009.05.013

Lieberman DE, Ross CF, Ravosa MJ (2000) The primate cranial base: ontogeny, function, and integration. Am J Phys Anthropol Suppl 31:117–169

Liedigk R, Roos C, Brameier M, Zinner D (2014) Mitogenomics of the Old World monkey tribe Papionini. BMC Evol Biol 14:176. https://doi.org/10.1186/s12862-014-0176-1

Maschenko EN (1994) Papio (Paradolichopithecus) suschkini (Trofimov): A revision of systematics, morphofunctional peculiarities of the skull and mandible. Paleotheriology. Nauka, Moscow, pp 15–57

Maschenko EN (2005) Cenozoic primates of eastern Eurasia (Russia and adjacent areas). Anthropol Sci 113:103–115. https://doi.org/10.1537/ase.04S015

Mitteroecker P, Gunz P, Bernhard M, Schaefer K, Bookstein FL (2004) Comparison of cranial ontogenetic trajectories among great apes and humans. J Hum Evol 46:679–697. https://doi.org/10.1016/j.jhevol.2004.03.006

Mouri T (1994) Postnatal growth and sexual dimorphism in the skull of the Japanese macaque (Macaca fuscata). Anthropol Sci 102:43–56. https://doi.org/10.1537/ase.102.Supplement_43

Nishimura TD, Takai M, Maschenko EN (2007) The maxillary sinus of Paradolichopithecus sushkini (late Pliocene, southern Tajikistan) and its phyletic implications. J Hum Evol 52:637–646. https://doi.org/10.1016/j.jhevol.2006.12.004

Nishimura TD, Senut B, Prieur A, Treil J, Takai M (2009) Nasal architecture of Paradolichopithecus arvernensis (late Pliocene, Seneze, France) and its phyletic implications. J Hum Evol 56:213–217. https://doi.org/10.1016/j.jhevol.2008.10.002

Nishimura TD, Ito T, Yano W, Ebbestad JOR, Takai M (2014) Nasal architecture in Procynocephalus wimani (Early Pleistocene, China) and implications for its phyletic relationship with Paradolichopithecus. Anthropol Sci 122:101–113. https://doi.org/10.1537/ase.140624

O'Higgins P, Collard M (2002) Sexual dimorphism and facial growth in papionin monkeys. J Zool 257:255–272. https://doi.org/10.1017/S0952836902000857

O'Higgins P, Jones N (1998) Facial growth in Cercocebus torquatus: an application of three-dimensional geometric morphometric techniques to the study of morphological variation. J Anat 193:251–272. https://doi.org/10.1046/j.1469-7580.1998.19320251.x

Pan R-L, Oxnard C (2000) Craniodental variation of macaques (Macaca): size, function and phylogeny. Zool Res 21:308–322. https://doi.org/10.1186/1471-2148-2-10

Penin X, Berge C, Baylac M (2002) Ontogenetic study of the skull in modern humans and the common chimpanzees: neotenic hypothesis reconsidered with a tridimensional Procrustes analysis. Am J Phys Anthropol 118:50–62. https://doi.org/10.1002/ajpa.10044

Perelman P et al (2011) A molecular phylogeny of living primates. PLoS Genet 7:e1001342. https://doi.org/10.1371/journal.pgen.1001342

Plavcan JM, van Schaik C (1994) Canine dimorphism. Evol Anthropol 2:208–214

Plavcan JM, van Schaik CP, Kappeler PM (1995) Competition, coalitions and canine size in primates. J Hum Evol 28:245–276. https://doi.org/10.1006/jhev.1995.1019

Pozzi L, Hodgson JA, Burrell AS, Sterner KN, Raaum RL, Disotell TR (2014) Primate phylogenetic relationships and divergence dates inferred from complete mitochondrial genomes. Mol Phylogenet Evol 75:165–183. https://doi.org/10.1016/j.ympev.2014.02.023

Pugh KD, Gilbert CC (2018) Phylogenetic relationships of living and fossil African papionins: combined evidence from morphology and molecules. J Hum Evol 123:35–51. https://doi.org/10.1016/j.jhevol.2018.06.002

Raaum RL, Sterner KN, Noviello CM, Stewart CB, Disotell TR (2005) Catarrhine primate divergence dates estimated from complete mitochondrial genomes: concordance with fossil and nuclear DNA evidence. J Hum Evol 48:237–257. https://doi.org/10.1016/j.jhevol.2004.11.007

R Development Core Team (2016) R: a language and environment for statistical computing. R Foundation for Statistical Computing, Vienna. https://www.R-project.org/

Roberts P, Delson E, Miracle P, Ditchfield P, Roberts RG, Jacobs Z, Blinkhorn J, Ciochon RL, Fleagle JG, Frost SR, Gilbert CC, Gunnell GF, Harrison T, Korisettar R, Petraglia MD (2014) Continuity of mammalian fauna over the last 200,000 y in the Indian subcontinent. Proc Nat Acad Sci 111(16):5848–5853

Roos C, Kothe M, Alba DM, Delson E, Zinner D (2019) The radiation of macaques out of Africa: evidence from mitogenome divergence times and the fossil record. J Hum Evol 133:114–132. https://doi.org/10.1016/j.jhevol.2019.05.017

Ross CF, Ravosa MJ (1993) Basicranial flexion, relative brain size, and facial kyphosis in nonhuman primates. Am J Phys Anthropol 91:305–324. https://doi.org/10.1002/ajpa.1330910306

Schlager S (2017) Morpho and Rvcg—shape analysis in R. In: Zheng G, Li S, Szekely G (eds) Statistical shape and deformation analysis. Academic Press, pp 217–256

Shea BT (1983) Size and diet in the evolution of African ape craniodental form. Folia Primatol 40:32–68. https://doi.org/10.1159/000156090

Singleton M (2002) Patterns of cranial shape variation in the Papionini (Primates: cercopithecinae). J Hum Evol 42:547–578. https://doi.org/10.1006/jhev.2001.0539

Singleton M (2004) Geometric morphometric analysis of functional divergence in mangabey facial form. J Anthropol Sci 82:27–44

Singleton M (2012) Postnatal cranial development in papionin primates: an alternative model for hominin evolutionary development. Evol Biol 39:499–520. https://doi.org/10.1007/s11692-011-9153-4

Springer MS et al (2012) Macroevolutionary dynamics and historical biogeography of primate diversification inferred from a species supermatrix. PLoS One 7:e49521. https://doi.org/10.1371/journal.pone.0049521

Strasser E, Delson E (1987) Cladistic analysis of cercopithecid relationships. J Hum Evol 16:81–99. https://doi.org/10.1016/0047-2484(87)90061-3

Szalay FS, Delson E (1979) Evolutionary history of the primates. Academic Press, New York

Takai M, Maschenko EN, Nishimura TD, Anezaki T, Suzuki T (2008) Phylogenetic relationships and biogeographic history of Paradolichopithecus sushkini Trofimov 1977, a large-bodied cercopithecine monkey from the Pliocene of Eurasia. Quat Int 179:108–119. https://doi.org/10.1016/j.quaint.2007.10.012

Takenaka O, Hotta M, Kawamoto Y, Suryobroto B, Brotoisworo E (1987) Origin and evolution of the Sulawesi macaques. 2. complete amino-acid-sequences of 7 Bbeta-chains of 3 molecular types. Primates 28:99–109. https://doi.org/10.1007/Bf02382187

Tosi AJ, Morales JC, Melnick DJ (2000) Comparison of Y chromosome and mtDNA phylogenies leads to unique inferences of macaque evolutionary history. Mol Phylogenet Evol 17:133–144. https://doi.org/10.1006/mpev.2000.0834

Tosi AJ, Disotell TR, Morales JC, Melnick DJ (2003) Cercopithecine Y-chromosome data provide a test of competing morphological evolutionary hypotheses. Mol Phylogenet Evol 27:510–521. https://doi.org/10.1016/S1055-7903(03)00024-1

Williams FL, Ackermann RR, Leigh SR (2007) Inferring Plio-Pleistocene southern African biochronology from facial affinities in Parapapio and other fossil papionins. Am J Phys Anthropol 132:163–174. https://doi.org/10.1002/ajpa.20504

Wickham H (2016) ggplot2: elegant graphics for data analysis. Springer-Verlag, New York

Zollikofer CPE, Ponce de León MS (2002) Visualizing patterns of craniofacial shape variation in Homo sapiens. Proc Biol Sci 269:801–807. https://doi.org/10.1098/rspb.2002.1960